however, the protease sensitivity increases under alkali conditions (*5*, *34*). These transmembrane peptide portions, classified as "category 2," are shielded from the lipid bilayer by other membrane peptide portions, and peptide-peptide interactions occur (*5*, *6*). These portions are more flexible than typical transmembrane segments that interact with lipids, and must be important for a transporter mechanism induced by conformational changes (*35*). Other chemical anion transport inhibitors that attack Lys 851 (*21*, *22*), Glu 681 (*20*) and His 834 (*23*) are concentrated in category 2 peptide portions (*34*). Especially, His 834 play an essential role in the conformational change that occurs during band 3 mediated anion transport (*23*). As discussed above, Lys 590 has a role in regulating anion transport activity and allosteric interactions with the anion binding site. These findings support our idea that the "category 2" peptide portions, including that containing Lys 590 in TM 6, play an important role in the anion transport mechanism (*5*, *6*, *35*).

An interesting result was obtained in the case of tryptic peptides of the transmembrane domain of band 3 modified by SITS. Trypsin cleavable sites on band 3, Arg 384, Arg 387, Arg 388, Arg 389, Arg 432 and Lys 430, were all susceptible to trypsin when band 3 was not modified by SITS (*5*, *34*). When band 3 was covalently modified with SITS, all these trypsin cleavable sites became resistant and a 22-kDa fragment (from Gly 361 to Lys 551) was recovered from the SITS-modified membranes even though the membranes were extensively digested with trypsin (see Fig. 2B, peak a in Fig. 6A and Table 3). The same 22-kDa fragment peak (peak a in Fig. 6A) was also recovered from SITS-modified membranes when the membranes were digested with trypsin, chymotrypsin or proteinase K (data not shown), indicating that a region of band 3 including the 22-kDa fragment is resistant to proteinases when band 3 is covalently modified by SITS. We have shown that the N-terminal region of the transmembrane domain of band 3 is essential for the anion transport activity (*36*), and that the N-terminal region of the membrane domain (from Gly 361 to Ala 408) interacts with the loop between TM 13 and TM 14 (*34*). These regions are hidden from the cytoplasmic surface when band 3 takes the outward conformation (Takazaki *et al.*, unpublished data). It has been shown that DIDS stabilizes the band 3 conformation (*37*) and that stilbene compounds such as DIDS and SITS alter the band 3 conformation from the inward to the outward conformation (*38*, *39*). Previous studies have suggested that band 3 contains subdomains comprising TM 1–5, TM 6–8, and TM 9–12 that interact with each other (*5*, *6*, *34*, *40*). The present results indicate that the 22-kDa fragment region including TM 1–5 (from Ser 401 to Phe 544) forms a subdomain of band 3, and that the subdomain is resistant to proteinases *in situ* when SITS binds covalently to band 3. Although DNFB also binds to the same Lys 539 as SITS, DNFB does not stabilize the 22-kDa fragment region.

In conclusion, we present here an analytical method for use with erythrocyte membrane proteins. The method comprising amino acid sequencing, MALDI-TOF and LC/ESI-MS is useful for the molecular study of band 3 and other minor membrane proteins in erythrocyte membranes. Furthermore we determined the important residues in band 3 for anion transport by identifying the chemically modified sites, and these residues play essential roles in anion transport mechanism. These findings will promote a better understanding of membrane protein structure and function relationships.

This work was supported in part by Grants-in-Aid for Scientific Research from the Ministry of Education, Science, Sports, and Culture of Japan (N.H. and Y.A.), and a grant from Kaibara Foundation (Y.A.).

REFERENCES

1. Iwata, S., Ostermeier, C., Ludwig, B., Michel, H., and Low, P.S. (1995) Structure at 2.8 A resolution of cytochrome c oxidase from Paracoccus denitrificans. *Nature* **376**, 660–669
2. Chang, G. and Roth, C.B. (2001) Structure of MsbA from E. coli: a homolog of the multidrug resistance ATP binding cassette (ABC) transporters. *Science* **293**, 1793–1800
3. Sui, H., Han, B.G., Lee, J.K., Walian, P., and Jap, B.K. (2001) Structural basis of water-specific transport through the AQP1 water channel. *Nature* **414**, 872–878
4. Abramson, J., Smirnova, I., Kasho, V., Verner, G., Kaback, H.R., and Iwata, S. (2003) Structure and mechanism of the lactose permease of Escherichia coli. *Science* **301**, 610–615
5. Hamasaki, N., Okubo, K., Kuma, H., Kang, D., and Yae, Y. (1997) Proteolytic cleavage sites of band 3 protein in alkali-treated membranes: fidelity of hydropathy prediction for band 3 protein. *J. Biochem.* **122**, 577–585
6. Hamasaki, N., Kuma, H., Ota, K., Sakaguchi, M., and Mihara, K. (1998) A new concept in polytopic membrane proteins following from the study of band 3 protein. *Biochem. Cell Biol.* **76**, 729–733
7. Ott, C.M., and Lingappa, V.R. (2002) Integral membrane protein biosynthesis: why topology is hard to predict. *J. Cell Sci.* **115**, 2003–2009
8. Santoni, V., Kieffer, S., Desclaux, D., Masson, F., and Rabilloud, T. (2000) Membrane proteomics: use of additive main effects with multiplicative interaction model to classify plasma membrane proteins according to their solubility and electrophoretic properties. *Electrophoresis* **21**, 3329–3344
9. Low, T.Y., Seow, T.K., and Chung, M.C. (2002) Separation of human erythrocyte membrane associated proteins with one-dimensional and two-dimensional gel electrophoresis followed by identification with matrix-assisted laser desorption/ionization-time of flight mass spectrometry. *Proteomics* **2**, 1229–1239
10. Kopito, R.R. and Lodish, H.F. (1985) Primary structure and transmembrane orientation of the murine anion exchange protein. *Nature* **316**, 234–238
11. Lux, S.E., John, K.M., Kopito, R.R., and Lodish, H.F. (1989) Cloning and characterization of band 3, the human erythrocyte anion- exchange protein. (AE1) *Proc. Natl Acad. Sci. USA* **86**, 9089–9093
12. Tanner, M.J., Martin, P.G., and High, S. (1988) The complete amino acid sequence of the human erythrocyte membrane anion-transport protein deduced from the cDNA sequence. *Biochem. J.* **256**, 703–712
13. Wood, P.G. (1992) in The anion exchange proteins: Homology and secondery structure. *Progress in Cell Res.* Vol. **2**, pp. 325–352, Elsevier Science Publishers, Amsterdam
14. Lepke, S. and Passow, H. (1976) Effects of incorporated trypsin on anion exchange and membrane proteins in human red blood cell ghosts. *Biochim. Biophys. Acta* **455**, 353–370
15. Lepke, S., Becker, A., and Passow, H. (1992) Mediation of inorganic anion transport by the hydrophobic domain of mouse erythroid band 3 protein expressed in oocytes of Xenopus laevis. *Biochim. Biophys. Acta* **1106**, 13–16
16. Izuhara, K., Okubo, K., and Hamasaki, N. (1989) Conformational change of band 3 protein induced by diethyl pyrocarbonate modification in human erythrocyte ghosts. *Biochemistry* **28**, 4725–4728

17. Jennings, M.L. and Anderson, M.P. (1987) Chemical modification and labeling of glutamate residues at the stilbenedisulfonate site of human red blood cell band 3 protein. *J. Biol. Chem.* **262**, 1691–1697
18. Zaki, L. (1981) Inhibition of anion transport across red blood cells with 1, 2-cyclohexanedione. *Biochem. Biophys. Res. Commun.* **99**, 243–251
19. Wood, P.G., Muller, H., Sovak, M., and Passow, H. (1992) Role of Lys 558 and Lys 869 in substrate and inhibitor binding to the murine band 3 protein: a study of the effects of site-directed mutagenesis of the band 3 protein expressed in the oocytes of Xenopus laevis. *J. Membr. Biol.* **127**, 139–148
20. Passow, H., Karbach, D., Aranibar, N., Liebold, K., Wood, P.G., and Lepke, S. (1996) *Membrane Proteins Structure Function and Expression Control* (Hamasaki, N. and Mihara, K., eds.), pp. 373–404, Kyushu University Press, Fukuoka
21. Okubo, K., Kang, D., Hamasaki, N., and Jennings, M.L. (1994) Red blood cell band 3. Lysine 539 and lysine 851 react with the same H_2DIDS (4, 4'-diisothiocyanodihydrostilbene-2, 2'-disulfonic acid) molecule. *J. Biol. Chem.* **269**, 1918–1926
22. Kawano, Y., Okubo, K., Tokunaga, F., Miyata, T., Iwanaga, S., and Hamasaki, N. (1988) Localization of the pyridoxal phosphate binding site at the COOH- terminal region of erythrocyte band 3 protein. *J. Biol. Chem.* **263**, 8232–8238
23. Jin, X.R., Abe, Y., Li, C.Y., and Hamasaki, N. (2003) Histidine-834 of human erythrocyte band 3 has an essential role in the conformational changes that occur during the band 3-mediated anion exchange. *Biochemistry* **42**, 12927–12932
24. Kang, D., Okubo, K., Hamasaki, N., Kuroda, N., and Shiraki, H. (1992) A structural study of the membrane domain of band 3 by tryptic digestion. Conformational change of band 3 *in situ* induced by alkali treatment. *J. Biol. Chem.* **267**, 19211–19217
25. Casey, J.R., Lieberman, D.M., and Reithmeier, R.A. (1989) Purification and characterization of band 3 protein. *Methods Enzymol.* **173**, 494–512
26. Rudloff, V., Lepke, S., and Passow, H. (1983) Inhibition of anion transport across the red cell membrane by dinitrophenylation of a specific lysine residue at the H_2DIDS binding site of the band 3 protein. *FEBS Lett.* **163**, 14–21
27. Eng, J.K., McCormack, A.L., and Yates, J.R. 3rd. (1994) An approach to correlate tandem mass apwctral data of peptides with amino acid sequences in a protein database. *J. Amer. Soc. Mass Spectrom.* **5**, 976–989
28. Laemmli, U.K. (1970) Cleavage of structural proteins during the assembly of the head of bacteriophage T4. *Nature* **227**, 680–685
29. Kawano, Y. and Hamasaki, N. (1986) Isolation of a 5, 300-dalton peptide containing a pyridoxal phosphate binding site from the 38, 000-dalton domain of band 3 of human erythrocyte membranes. *J. Biochem.* **100**, 191–199
30. Lowry, O.H., Rosebrough, N.J., Farr, A.L., and Randall, R.J. (1951) Protein measurement with Folin phenol reagent. *J. Biol. Chem.* **193**, 265–275
31. Passow, H., Lepke, S., and Wood, P.G. (1992) *The Band 3 Proteins:Anion Transporters, Binding Proteins and Senescent Antigens., Progress in Cell Res.*, Vol. **2**, pp. 85–98, Elsevier Science Publishers, Amsterdam
32. Melchior, W.B., Jr. and Fahrney, D. (1970) Ethoxyformylation of proteins. Reaction of ethoxyformic anhydride with alpha-chymotrypsin, pepsin, and pancreatic ribonuclease at pH 4. *Biochemistry* **9**, 251–258
33. Brock, C.J., Tanner, M.J., and Kempf, C. (1983) The human erythrocyte anion-transport protein. Partial amino acid sequence, conformation and a possible molecular mechanism for anion exchange. *Biochem. J.* **213**, 577–586
34. Kuma, H., Abe, Y., Askin, D., Bruce, L.J., Hamasaki, T., Tanner, M.J., and Hamasaki, N. (2002) Molecular basis and functional consequences of the dominant effects of the mutant band 3 on the structure of normal band 3 in Southeast Asian ovalocytosis. *Biochemistry* **41**, 3311–3320
35. Hamasaki, N., Abe, Y., and Tanner, M.J. (2002) Flexible regions within the membrane-embedded portions of polytopic membrane proteins. *Biochemistry* **41**, 3852–3854
36. Kanki, T., Young, M.T., Sakaguchi, M., Hamasaki, N., and Tanner, M.J. (2003) The N-terminal region of the transmembrane domain of human erythrocyte band 3. Residues critical for membrane insertion and transport activity. *J. Biol. Chem.* **278**, 5564–5573
37. Davio, S.R. and Low, P.S. (1982) Characterization of the calorimetric C transition of the human erythrocyte membrane. *Biochemistry* **21**, 3585–3593
38. Barzilay, M., Ship, S., and Cabantchik, Z.I. (1979) Anion transport in red blood cells. I. Chemical properties of anion recognition sites as revealed by structure-activity relationships of aromatic sulfonic acids. *Membr. Biochem.* **2**, 227–254
39. Shami, Y., Rothstein, A., Knauf, P.A., Jennings, M.L., and Anderson, M.P. (1978) Identification of the Cl- transport site of human red blood cells by a kinetic analysis of the inhibitory effects of a chemical probe. *Biochim. Biophys. Acta* **508**, 357–363
40. Groves, J.D. and Tanner, M.J. (1999) Structural model for the organization of the transmembrane spans of the human red-cell anion exchanger (band 3; AE1). *Biochem. J.* **344**, 699–711
41. Hirokawa, T., Boon-Chieng, S., and Mitaku, S. (1998) SOSUI: Classification and secondary structure prediction system for membrane proteins. *Bioinformatics* **14**, 378–379

Clinical Chemistry 50:11
2045–2051 (2004)

High-Sensitivity Detection of the A3243G Mutation of Mitochondrial DNA by a Combination of Allele-Specific PCR and Peptide Nucleic Acid-Directed PCR Clamping

MICHIYO URATA,[1] YUI WADA,[1] SANG HO KIM,[1,2] WORAWAN CHUMPIA,[1,3] YUZO KAYAMORI,[1] NAOTAKA HAMASAKI,[1] and DONGCHON KANG[1*]

Background: **The A3243G mutation of mitochondrial DNA (mtDNA) is involved in many common diseases, including diabetes mellitus and mitochondrial encephalomyopathy with lactic acidosis and stroke-like episodes (MELAS). For detection of this mutation, allele-specific PCR is highly sensitive but requires strict control of PCR conditions; it thus is not adequate for a routine clinical test. We aimed to develop a routinely available PCR method for quantitative detection of low-level heteroplasmy of the A3243G mutation.**

Methods: **Quantitative allele-specific PCR for the A3243G mutation was performed in the presence of peptide nucleic acid (PNA), in which PNA is complementary to the wild-type mtDNA, with one primer having a 3′ end matched to nucleotide position 3243 of the mutant.**

Results: **With our method, amplification of wild-type mtDNA was suppressed 7000-fold compared with amplification of the mutant mtDNA under a broad range of conditions: DNA, 5–100 ng; annealing temperature, 61–66 °C; and PNA, 1.5–3.5 μmol/L. Hence, 0.1% heteroplasmy of the A3243G mutation can be reliably quantified by this method. Blood samples form 40 healthy volunteers showed <0.06% heteroplasmy, suggesting that 0.1% is diagnostically significant.**

Conclusions: **PNA maintains the specificity of allele-specific PCR over a wide range of conditions, which is important for routine clinical testing.**

All vertebrate mitochondria have semi-autonomously replicating extranuclear genomes. Human mitochondrial DNA (mtDNA)[4] encodes 13 subunits of the mitochondrial respiratory chain, 22 tRNAs, and 2 rRNAs, all of which are essential for assembly of the mitochondrial respiratory chain that produces most of the cellular ATP. Inherited mtDNA mutations have been associated with a variety of neuromuscular disorders *(1)*. More than 100 different mtDNA mutations have been reported to be related to various disorders, and that number is still increasing *(1)*. Because a cell may contain hundreds to thousands of mtDNA molecules, heteroplasmy (coexistence of wild-type and mutant mtDNA in a single cell) is usually present in mitochondrial diseases. Disease symptoms appear only when the percentage of mutant mtDNA exceeds a particular value (threshold). It is therefore common to find that affected tissues show a high percentage of the specific heteroplasmy, whereas other, apparently unaffected cells in the same individual have much lower percentages of the heteroplasmy or show no detectable mutations at that site.

Mitochondrial mutations are broadly classified into two groups: rearrangements (deletions and duplications) and point mutations. Among point mutations, an A-to-G

[1] Department of Clinical Chemistry and Laboratory Medicine, Kyushu University, Graduate School of Medical Sciences, Fukuoka, Japan.
[2] Department of Biology Education, Daegue University, Kyungsan, Korea.
[3] Thalassemia Research Center, Institute of Science and Technology for Research and Development, Mahidol University, Nakornpathom, Thailand.
*Address correspondence to this author at: Department of Clinical Chemistry and Laboratory Medicine, Kyushu University Graduate School of Medical Sciences, 3-1-1 Maidashi Higashi-ku, Fukuoka 812-8582, Japan. Fax 81-92-642-5772; e-mail kang@mailserver.med.kyushu-u.ac.jp.
Received March 4, 2004; accepted August 19, 2004.
Previously published online at DOI: 10.1373/clinchem.2004.033761

[4] Nonstandard abbreviations: mtDNA, mitochondrial DNA; np, nucleotide position; MELAS, mitochondrial encephalomyopathy with lactic acidosis and stroke-like episodes; DM, diabetes mellitus; RFLP, restriction fragment length polymorphism; LMPCR, ligation-mediated PCR; PNA, peptide nucleic acid; T_m, melting temperature; and SNP, single-nucleotide polymorphism.

mutation at nucleotide position (np) 3243 in the human mitochondrial $tRNA^{Leu}$(UUR) gene (A3243G) is the most common. This particular mutation accounts for ~80% of patients with mitochondrial encephalomyopathy with lactic acidosis and stroke-like episodes (MELAS) *(2, 3)*. The percentage of cells containing mtDNA with the heteroplasmic A3243G mutation varies from tissue to tissue as described above and may be highest in affected tissues such as muscle and brain. However, samples that may be easily attained in a noninvasive manner and routinely used, such as blood or urinary cells, usually show lower percentages of heteroplasmy. For example, the A3243G mutation was detected in the blood of only 5 of 10 patients but was detected in the muscle of all 10 patients *(4)*.

In addition to the classic mitochondrial encephalomyopathies such as MELAS, the A3243G mtDNA mutation has been shown to be involved type II diabetes mellitus (DM) and aging *(5)*. Normal ATP production in mitochondria is critical, particularly for insulin secretion from pancreatic beta cells *(6)*. Consistent with this fact, individuals with various types of MELAS often have symptoms of diabetes *(7, 8)*, and accumulation of the mutation in pancreatic beta cells could cause adult-onset DM. In fact, the mutation is also found in patients with DM who were not previously diagnosed with MELAS *(9)*. Although many of these patients exhibit a variety of neurologic disorders, typically including deafness, the A3243G mutation has also been found in DM patients with few neuromuscular symptoms. Considering that the heteroplasmy may be highest in affected tissues, the pancreas may be a good source for examination of the A3243G mutation in patients with diabetes *(10)*; however, pancreatic biopsy is not available for routine screening. Instead, peripheral leukocytes and urinary epithelial cells, which are obtained in a noninvasive manner, are commonly used in screening. The percentage of mtDNA mutations is usually higher in the latter than in the former *(11–13)*.

The A3243G mutation creates a new restriction site for the restriction enzyme *ApaI*; thus, this mutation is typically surveyed by a conventional PCR-restriction fragment length polymorphism (RFLP) method in which a region including np 3243 is PCR-amplified, digested with *ApaI*, and then stained with ethidium bromide after agarose gel electrophoresis. This method can barely detect the heteroplasmy at concentrations of 5–10% *(14)*. Although the prevalence of DM patients with the A3243G mutation is estimated to be 1–2% of all DM patients *(8)*, it is highly likely that the A3243G mutation will be missed in some DM patients by the RFLP method using peripheral blood cells *(14, 15)*. To address this issue, we previously developed a sensitive ligation-mediated PCR-based (LMPCR) method that is able to detect the A3243G heteroplasmy present at a concentration of 0.01% *(16)*. With the LMPCR method, we were able to detect the heteroplasmy present at 0.01–0.1% in approximately one-half of 136 apparently healthy volunteers; no volunteer had more than 0.1%. On the other hand, we found that the heteroplasmy was present in concentrations >0.1% in the leukocytes of 1% of 233 patients with type II DM.

This LMPCR method is very specific and highly sensitive, but it is only semiquantitative, in addition to being somewhat laborious and time-consuming. Thus, it is not an ideal routine clinical test, especially for large numbers of samples. We developed a sensitive quantitative method that combines peptide nucleic acid (PNA) and allele-specific PCR (Fig. 1, bottom panel). This combination increases the detection of the A3243 heteroplasmy by approximately two orders of magnitude more than use of PNA-directed PCR-clamping alone (Fig. 1, top panel).

Materials and Methods

BLOOD DONORS AND CELL LINES

Blood from 40 healthy donors who were mainly workers in the Kyushu University Hospital was collected in tubes containing 1.5 g/L disodium EDTA. The donors ranged in age from their twenties to their fifties [mean (SD) age, 38.7 (11.9) years] and included five males and five females in each 10-year age group. Blood sampling was performed after receipt of informed consent according to the ethics guidelines of the Kyushu University Hospital. Two cybrid

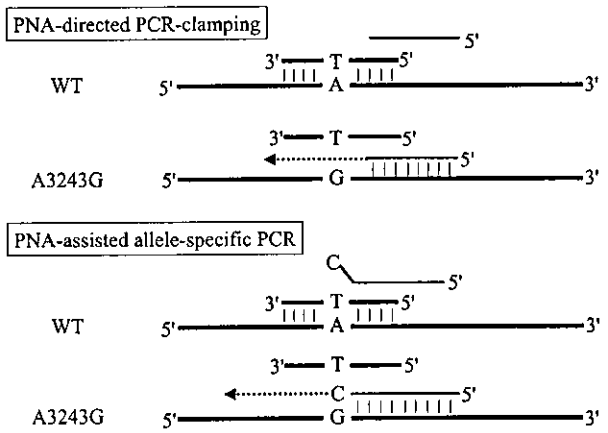

Fig. 1. Schemes for PNA-directed PCR clamping and PNA-assisted allele-specific PCR.

The L-strand of mtDNA around 3243 is shown as a *thick black line*. The 3243 site is shown only by a nucleotide. *Thin black* and *thick gray lines* indicate a DNA primer and PNA, respectively. The *dotted arrow* denotes newly synthesized DNA. The PNA is designed to completely match a wild-type (*WT*) mtDNA region including np 3243 at its middle. In PNA-directed PCR-clamping (*top panel*), an antisense primer DNA is designed to partly overlap the PNA-binding region but not to reach np 3243. PNA usually binds to a DNA strand more strongly than does naturally occurring DNA; therefore, the PNA expels the 3′ side of the primer from wild-type mtDNA and inhibits the amplification of wild-type mtDNA. In general, one nucleotide mismatch makes the binding of PNA much weaker. Therefore, the primer instead of the PNA binds to 3243 mutant mtDNA, leading to amplification of the mutant mtDNA. In PNA-assisted allele-specific PCR (*bottom panel*), an antisense primer is designed to end at np 3243 and to match to the 3243 mutant. Because of this 3′ mismatch, the amplification of wild-type mtDNA is largely suppressed. In addition, because the PNA expels the 3′ side of the primer, the amplification of wild-type mtDNA is further inhibited. The PNA is more efficiently detached from the 3243 mutant mtDNA in PNA-assisted allele-specific PCR than in PNA-directed PCR clamping because the primer overlaps the PNA region longer in the former than in the latter.

cell lines carrying 100% wild-type and 100% A3243G mutant mtDNA (2SA and 2SD, respectively) were made by fusion of human mtDNA-deficient rho^0 206 cells and enucleated fibroblasts derived from a patient with A3243G MELAS *(17)*.

PREPARATION OF DNA

The total DNA of the cell lines and peripheral leukocytes was extracted with QIAamp DNA extraction reagents (QIAGEN). The DNA was treated with RNase A, extracted with phenol–chloroform (1:1 by volume), precipitated with ethanol, resolubilized in 20 μL of distilled water, and quantified based on the absorbance at 260 nm.

PNA-ASSISTED ALLELE-SPECIFIC PCR

PNA (5′-ACCGGGCTCTGCCAT-3′), which was designed to bind the L-strand, was obtained from FASMAC Co., Ltd. A sense primer, mtL1-1 (5′-CAT AAC ACA GCA AGA CGA GAA GAC CCT ATG G-3′), and an antisense primer, mt3243HC (5′-TTT TAT GCG ATT ACC GGG CC-3′), were used. The standard PCR reaction mixture consisted of 1× LightCycler mixture (LC-FastStart Reaction Mix SYBR GREEN I; Roche) containing the DNA-binding fluorescent dye SYBR Green I and *Taq* DNA polymerase, 2.5 μM PNA, 0.25 μM each primer, and 10 ng of total DNA in 20 μL. Thermal cycling was conducted in a LightCycler. The standard conditions were as follows: an initial DNA denaturation step of 10 min at 94 °C and an amplification step of 20 s at 94 °C, 5 s at 77 °C, 5 s at 70 °C, 10 s at 64 °C, and 20 s at 72 °C. The 5 s at 77 °C and 5 s at 70 °C steps were inserted to slow the temperature decrease and allow binding of PNA to DNA. DNA amplification was monitored in real time.

QUANTIFICATION OF mtDNA

An ~300-bp DNA fragment (np 16052–16361) was PCR-amplified with sense primer 5mt16052 (5′-CCA CCC AAG TAT TGA CTC ACC C-3′) and antisense primer 3mt339 (5′-CGA GAA GGG ATT TGA CTG TAA TG-3′). The PCR product was cloned into a TA vector, pQTmt. The plasmid was quantified by the absorbance at 260 nm and used as the calibrator for total mtDNA (wild-type and the A3243G mutant) quantification. The PCR reaction mixture for the quantification consisted of 1× LightCycler mixture, 2.0 mM $MgCl_2$, 0.5 μM each primer, and various amounts of the pQTmt plasmid in 20 μL. Thermal cycling was conducted in a LightCycler. The standard thermocycling conditions were as follows: an initial DNA denaturation step of 10 min at 95 °C and an amplification step of 15 s at 95 °C, 5 s at 60 °C, and 15 s at 72 °C.

Similarly, an ~560-bp DNA fragment including the A3243G mutation (np 2703–3262) was PCR-amplified with mtL1-1 and antisense primer mt3243HC (the same as for the allele-specific PCR) and cloned into a TA vector; we named this plasmid pQMmt and used it as the calibrator for the A3243G mutant.

Results and Discussion

DETERMINATION OF PCR CONDITIONS

We determined the optimum conditions for amplification of the A3243G mutant mtDNA in two human cell lines, 2SA and 2SD, which carry 100% wild-type and 100% A3243G mutant mtDNA, respectively. The two cell lines contained essentially the same copy number of mtDNA per total DNA (see the "Total" column in Table 1). When we performed allele-specific PCR in the presence of PNA using 10 ng of total DNA in 20 μL of the reaction mixture, the crossing point of 2SD was ~15 cycles earlier than that of 2SA (Fig. 2A). The final fluorescent intensity of SYBR Green I, which indicates the amount of double-stranded DNA, was ~30% lower in 2SA than in 2SD. We mixed the two total DNAs at various ratios (from 0.1% to 10% 2SD) and found that 2SA DNA with 0.1% 2SD added could be clearly distinguished from 100% 2SA (Fig. 2A). By constructing a calibration curve of crossing points vs percentage of 2SD (100% to 0.1%; Fig. 2B), we could estimate a 2SA concentration that corresponded to a mean (SD) of 0.014 (0.0008)% of 2SD (n = 3). Given that 2SA is 100% wild type, the amplification of wild-type mtDNA was apparently suppressed ~7000-fold compared with the A3243G mutant in this PNA-assisted allele-specific PCR. The PCR products at the endpoint of the reaction (i.e., after 50 cycles) are shown in Fig. 2C.

The PCR products for 2SD were found at their anticipated band length of ~560 bp (Fig. 2C, lane 1). However, in the case of 2SA, the 560-bp product was much less prominent, and a lower band that may be derived from the presence of "primer-dimers" was detected (Fig. 2C, lane 5). The lower band was also observed in the absence of mtDNA (Fig. 2C, lane 6). Notably, the lower primer-dimer band was hardly seen even in 0.1% 2SD (Fig. 2C, lane 4), suggesting that the primer-dimer is formed only when the amount of the mutant 3243 mtDNA is extremely low or absent. From these results, the erroneous amplification of wild-type mtDNA may actually be much lower than that estimated by the fluorescence. As shown in the melting curves of the PCR products (Fig. 2D), the 560-bp product and the primer-dimer were readily distin-

Table 1. Estimation of 3243 heteroplasmy.[a]

	Mean (SD) mtDNA copy number/ng total DNA		
	Total	Mutant	Heteroplasmy, %
100% 2SD	19.1 (1.4) × 10^4	18.6 (3.4) × 10^4	97.3 (10.4)
10% 2SD	17.5 (1.6) × 10^4	1.7 (0.5) × 10^4	9.7 (1.7)
100% 2SA	18.6 (1.6) × 10^4	31.3 (11.6)	0.013 (0.005)

[a] Conditions were as follows: 2.5 μM PNA, 10 ng of total DNA, and an annealing temperature of 64 °C. The copy numbers of total mtDNA and mutant mtDNA were measured as described in the *Materials and Methods*. Three independent experiments were performed, with each experiment containing three measuring points. The means in each experiment were averaged, and the result is presented as the mean (SD). The heteroplasmy was determined by mean values of total and mutant copy numbers in each independent experiment, and then those values were averaged.

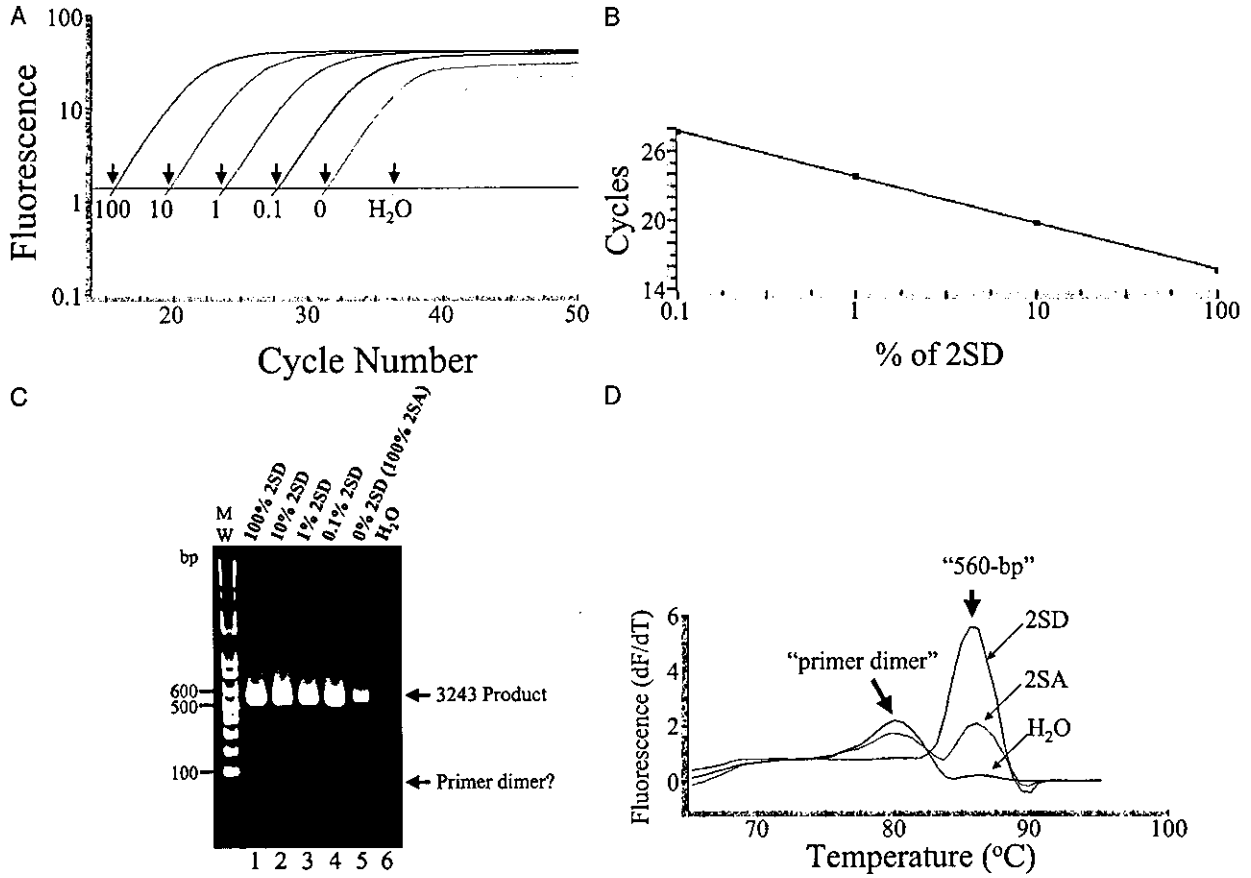

Fig. 2. Amplification of mtDNA carrying A3243G.

(*A*), total DNA from 2SD (100% mutant) and 2SA (100% wild type) cells was mixed and used for quantitative PCR of mtDNA carrying A3243G. The combined amount of DNA was 10 ng in the reaction mixture. The PNA concentration was 2.5 μM, and the annealing temperature was 64 °C. Each value *below* the *horizontal line* indicates the percentage of 2SD DNA, such that 0 (zero) indicates 100% 2SA. *H_2O* indicates that the PCR was done in the absence of DNA. *Arrows* indicate crossing points. (*B*), calibration curve for the crossing points against percentage of 2SD. (*C*), PCR products after 50 cycles were electrophoresed on a 1.0% agarose gel and stained with ethidium bromide. *Lane MW*, molecular markers. (*D*), melting curves of PCR products after 50 cycles. The fluorescence of PCR products is differentiated on the *y axis* (dF/d*T*) with respect to temperature. H_2O and 2SD showed a peak at 80 and 86 °C, respectively, whereas 2SA showed peaks at both of these temperatures.

guished, with the former having a higher melting temperature (T_m) than the latter (Fig. 2D).

We also examined whether this 15-cycle difference is maintained at different concentrations of total DNA. We varied the DNA amount from 1 to 100 ng. The 15-cycle difference was maintained between 5 and 100 ng (see Table 1 in the Data Supplement that accompanies the online version of this article at http://www.clinchem.org/content/vol50/issue11/). In addition, we changed the annealing temperatures from 60 °C to 68 °C. The 15-cycle difference was not affected much between 61 and 66 °C (Table 2 in the online Data Supplement). It is striking that the allele-specific PCR allows such a broad range of annealing temperatures because usually strict control of annealing temperatures is critical for assuring high specificity, particularly in cases with heteroplasmy <1%. Finally, we examined the effect of the PNA concentration. Without PNA, allele-specific PCR revealed an ~10-cycle difference between 2SA and 2SD, whereas the presence of PNA increased the difference by ~5 cycles (Table 3 in the online Data Supplement). These results suggest that allele-specific PCR plus PNA increases the specificity of amplification of the A3243G mutant by two orders of magnitude more than does PNA alone. The 15-cycle difference was observed with PNA concentrations between 1.5 and 3.5 μmol/L (Table 3 in the online Data Supplement).

DETERMINATION OF mtDNA COPY NUMBER

To quantitatively estimate the heteroplasmy, we determined the copy numbers of the mutant and total mtDNA. For the former, plasmid pQMmt, which includes a DNA fragment (np 2703–3262) containing the A3243G mutation was constructed and used as the copy number calibrator for the mutant mtDNA. We also added PNA in the PCR reaction mixtures for the calibration curve to adjust the

amplification efficiency of the mutant mtDNA. For the latter, plasmid pQTmt, which includes a DNA fragment (np 16052–16361), was constructed and used as the calibrator for determining copy number. Using these two plasmids, we measured the copy numbers of mutant and total mtDNA in 2SA and 2SD cells and then calculated the heteroplasmy. The heteroplasmy of 2SD cells was 97.3%, which is close to 100% (Table 1). The value for 2SA (0.013%) is consistent with the estimate that was obtained by mixing 2SA and 2SD (Fig. 2) and suggests that ~0.02% heteroplasmy is a background in this measurement system. The mixture of 2SA and 2SD DNA exhibited amounts of heteroplasmy close to the mixing ratio (Table 1).

We next measured the heteroplasmy in blood samples from 40 apparently healthy volunteers. When examining the specimens from the volunteers, we always measured 2SD in parallel. The obtained heteroplasmy value of the 2SD sample was divided by a factor and adjusted to 100%. For example, when the assay found 95% heteroplasmy for 2SD from the measured copy numbers of mutant and wild-type mtDNA, we divided the 95% by a factor of 0.95, and the same factor was applied to the values for the specimens to minimize measurement errors. When we used these techniques, no volunteer had more than 0.06% heteroplasmy [mean (SD), 0.03 (0.01)%]. We therefore concluded that finding 0.1% heteroplasmy is a reliable indication of the presence of the mutation.

We then tested this method with two MELAS patients, P1 and P2 (80% and 20% heteroplasmy, respectively, according to our method; Fig. 3A). The results of conventional PCR-RFLP analysis of those samples are shown in Fig. 3B. The results for patient P2 were markedly different from those for 2SA in the PNA-assisted allele-specific PCR assay (Fig. 3A), but the *Apa*I-cleaved bands in the sample from patient P2 were only weakly visible in the PCR-RFLP gel (Fig. 3B). The DNA from patient P1 was diluted 8-, 80-, and 800-fold with DNA of a healthy individual to make 10%, 1%, and 0.1% heteroplasmy, and the resulting theoretical 0.1% heteroplasmy was clearly distinguished from the DNA of a healthy volunteer (Fig. 3C). These results suggest that this new method is similarly sensitive for DNA extracted from peripheral blood cells from MELAS patients. We also examined 50 patients

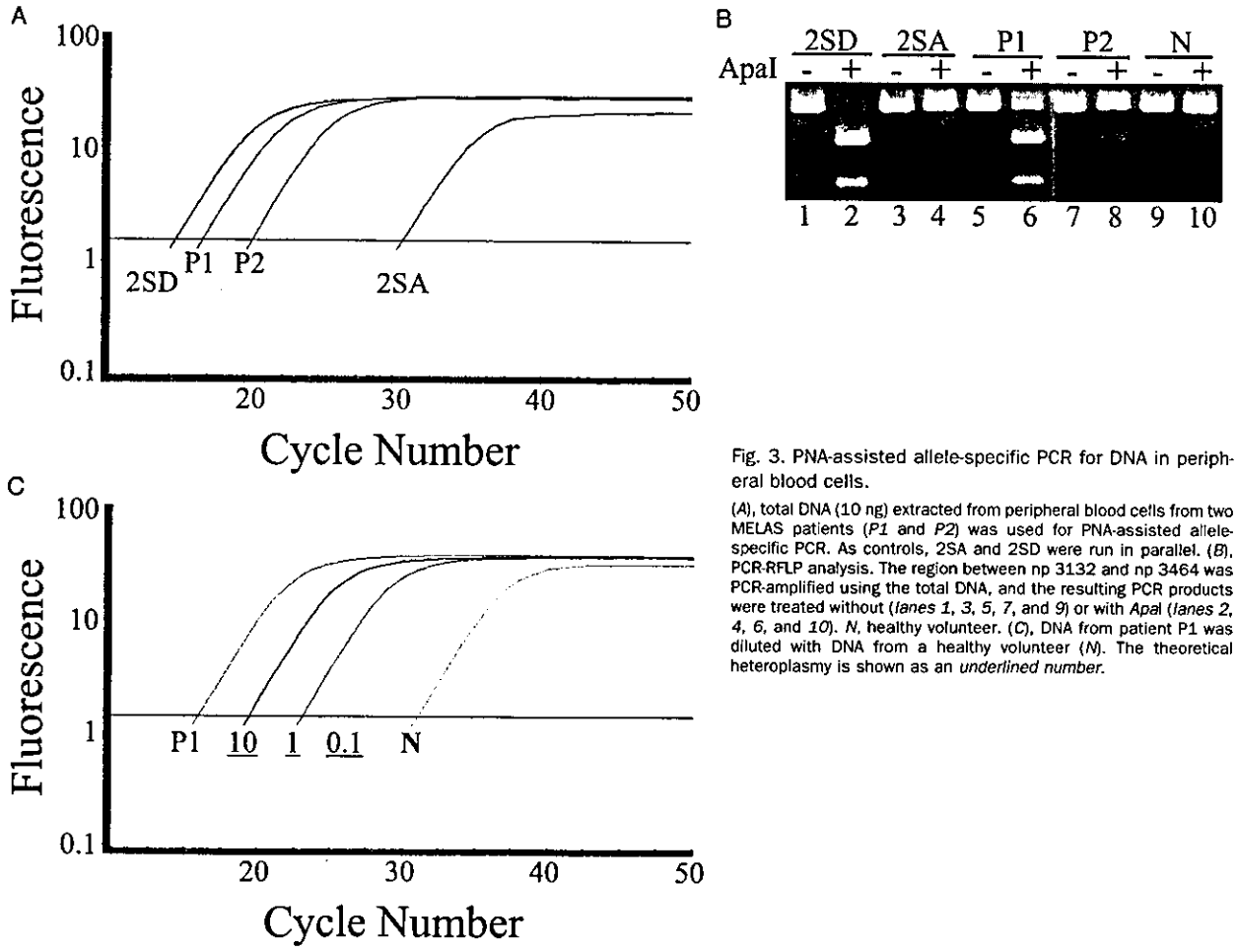

Fig. 3. PNA-assisted allele-specific PCR for DNA in peripheral blood cells.

(*A*), total DNA (10 ng) extracted from peripheral blood cells from two MELAS patients (*P1* and *P2*) was used for PNA-assisted allele-specific PCR. As controls, 2SA and 2SD were run in parallel. (*B*), PCR-RFLP analysis. The region between np 3132 and np 3464 was PCR-amplified using the total DNA, and the resulting PCR products were treated without (*lanes 1, 3, 5, 7,* and *9*) or with *Apa*I (*lanes 2, 4, 6,* and *10*). *N*, healthy volunteer. (*C*), DNA from patient P1 was diluted with DNA from a healthy volunteer (*N*). The theoretical heteroplasmy is shown as an *underlined number.*

with type II DM and found 2 positive individuals, with 20% and 40% heteroplasmy, respectively (results not shown).

Murdock et al. *(18)* have reported that 0.1% heteroplasmy of the A3243G mutation is detected by a PNA-directed PCR-clamping method. However, in their report, the PCR product for the mutation was barely detectable at a 1% concentration when wild-type and mutant DNA were mixed at 100:1. Thus, they needed to perform a second round of PCR to make the signals visible. In addition, digestion of the second-round PCR products with a restriction enzyme was required to confirm the presence of the mutation because wild-type mtDNA was significantly amplified even at 1% in their system. Hancock et al. *(19)* also reported detection of 0.1% heteroplasmy by PNA-directed PCR clamping. Similarly, they needed to sequence the PCR products to confirm the A3243G mutation and to ensure that no other mutation interfered with the PNA binding to the wild type. Initially, we also attempted simple PNA-directed PCR clamping under many conditions, but we never succeeded in completely selectively amplifying the mutant mtDNA, even at 1%; i.e., wild-type mtDNA was always significantly amplified. Thus, under the present conditions, it seems to be impossible to completely suppress the amplification of wild-type mtDNA with PNA alone when the heteroplasmy is 1% and the wild type is 99%. An advantage to using a primer that does not overlap the 3243 site (Fig. 1, top panel) is that amplification of the mutant mtDNA can be definitively confirmed by enzyme digestion or sequencing *(18, 19)*. However, in our PNA-assisted allele-specific PCR (Fig. 1, bottom panel), we did not take this approach because we wished to develop a simple but quantitative method that can be performed in a typical clinical laboratory. Our method provides high specificity over a broad range of PCR conditions. Especially striking is that selective amplification is maintained over a wide range of annealing temperatures. This is particularly important from the point of view of routine clinical tests because we frequently encounter the problem of undesirable amplification by allele-specific PCR as a result of small fluctuations in the annealing temperature in PCR instruments, particularly when we are trying to detect very low percentages of heteroplasmy. We believe that the simple addition of PNA to any allele-specific PCR may generally improve the stability of allele-specific amplification.

The T_m of PNA/DNA is usually reduced by one base mismatch much more than is that of wild-type DNA/DNA. The PNA-directed PCR clamping is strongly based on this principle. However, this strong dependence on base matching could create an adverse situation if there is single-nucleotide polymorphism (SNP) in the region of PNA clamping, such that the wild-type genome is falsely amplified. This is also true for our PNA-assisted allele-specific PCR, although it is not totally dependent on the T_m of PNA. Fortunately, we did not find any SNPs from np 3236 to np 3250, the clamping region of our PNA, in the databases of Ingman et al. (76 persons) *(20)*, Finnila et al. (192 persons) *(21)*, Kong et al. (48 persons) *(22)*, or Herrnstadt et al. (560 persons) *(23)*. No SNPs in this region are found in the Japanese database for ~1000 Japanese *(24)* or in the US database *(1)*. Thus, this region is well conserved, and SNPs in the region may be extremely rare. Two cases with Kearns–Sayre syndrome are reported to harbor mutations at 3249 and 3250, respectively *(1)*. For these cases, a false positive may be better than a false negative. A patient who has a false-positive result for A3243G would then receive further examination for confirmation.

In conclusion, we show that 0.1% heteroplasmy is reliably and quantitatively detected by PNA-assisted allele-specific PCR and that the value 0.1% is not simply the lower limit of detection. When we previously measured heteroplasmy by LMPCR, we detected 0.01% heteroplasmy in peripheral blood cells from approximately one half of the healthy individuals and DM patients, but no healthy individuals had >0.1% heteroplasmy *(16)*. This observation was confirmed by the method presented in this report. Murdock et al. *(18)* also reported that the A3243G mutation does not typically accumulate above 0.1% with age, even in muscle or brain. Therefore, the presence of heteroplasmy >0.1% may be diagnostically significant. It is well established that healthy people typically harbor very low concentrations of the A3243G heteroplasmy *(18, 25)*. Recently, the authors of a case study reported that the concentration of the 3243 mutation in peripheral blood cells of a patient with mitochondrial diabetes was 0.102% *(26)*. Thus, the quantitative detection of 0.1% heteroplasmy appears to be a required and sufficient prerequisite for a practical clinical test for the A3243G mutation. Our method feasibly satisfies this condition and thus may be suitable for a routine clinical test. Because collecting urine samples is less invasive than collecting blood and the concentration of mtDNA mutations is usually much higher in urine samples than in blood samples *(11–13)*, application of this method to urine samples may be even more useful as a routine clinical test.

We extend special thanks to an anonymous reviewer for kind and extensive editing of the manuscript. This work was supported in part by the Uehara Memorial Foundation, the Naito Foundation, and Grants-in-Aid for Scientific Research from the Ministry of Education, Science, Technology, Sports, and Culture of Japan.

References

1. Wallace DC, Lott MT. MITOMAP: a human mitochondrial genome database. http://www.mitomap.org (accessed May 2004).
2. Liang MH, Wong LJ. Yield of mtDNA mutation analysis in 2,000 patients. Am J Med Genet 1998;77:395–400.

3. Wong LJ, Senadheera D. Direct detection of multiple point mutations in mitochondrial DNA. Clin Chem 1997;43:1857–61.
4. Sue CM, Quigley A, Katsabanis S, Kapsa R, Crimmins DS, Byrne E, et al. Detection of MELAS A3243G point mutation in muscle, blood and hair follicles. J Neurol Sci 1998;161:36–9.
5. Kang D, Hamasaki N. Mitochondrial oxidative stress and mitochondrial DNA. Clin Chem Lab Med 2003;41:1281–8.
6. Wollheim CB. Beta-cell mitochondria in the regulation of insulin secretion: a new culprit in type II diabetes. Diabetologia 2000;43: 265–77.
7. Rotig A, Bonnefont J-P, Munnich A. Mitochondrial diabetes mellitus. Diabetes Metab 1996;22:291–8.
8. Gerbitz K-D, van den Ouweland JMW, Maassen JA, Jaksch M. Mitochondrial diabetes: a review. Biochim Biophys Acta 1995; 1271:253–60.
9. Kadowaki T, Kadowaki H, Mori Y, Tobe K, Sakuta R, Suzuki Y, et al. A subtype of diabetes mellitus associated with a mutation of mitochondrial DNA. N Engl J Med 1994;330:962–8.
10. Kobayashi T, Nakanishi K, Nakase H, Kajio H, Okubo M, Murase T, et al. In situ characterization of islets in diabetes with a mitochondrial DNA mutation at nucleotide position 3243. Diabetes 1997;46:1567–71.
11. Hotta O, Inoue CN, Miyabayashi S, Furuta T, Takeuchi A, Taguma Y. Clinical and pathologic features of focal segmental glomerulosclerosis with mitochondrial tRNALeu(UUR) gene mutation. Kidney Int 2001;59:1236–43.
12. Nishigaki Y, Tadesse S, Bonilla E, Shungu D, Hersh S, Keats BJ, et al. A novel mitochondrial tRNA(Leu(UUR)) mutation in a patient with features of MERRF and Kearns-Sayre syndrome. Neuromuscul Disord 2003;13:334–40.
13. Puomila A, Viitanen T, Savontaus ML, Nikoskelainen E, Huoponen K. Segregation of the ND4/11778 and the ND1/3460 mutations in four heteroplasmic LHON families. J Neurol Sci 2002;205: 41–5.
14. Smith ML, Hua X-Y, Marsden DL, Liu D, Kennaway NG, Ngo K-Y, et al. Diabetes and mitochondrial encephalomyopathy with lactic acidosis and stroke-like episodes (MELAS): radiolabeled polymerase chain reaction is necessary for accurate detection of low percentages of mutation. J Clin Endocrinol Metab 1997;82: 2816–31.
15. Suzuki Y, Goto Y, Taniyama M, Nonaka I, Murakami N, Hosokawa K, et al. Muscle histopathology in diabetes mellitus associated with mitochondrial tRNALeu(UUR) mutation at position 3243. J Neurol Sci 1997;145:49–53.
16. Urata M, Wakiyama M, Iwase M, Yoneda M, Kinoshita S, Hamasaki N, et al. New sensitive method for the detection of the A3243G mutation of human mitochondrial deoxyribonucleic acid in diabetes mellitus patients by ligation-mediated polymerase chain reaction. Clin Chem 1998;44:2088–93.
17. Yoneda M, Miyatake T, Attardi G. Complementation of mutant and wild-type human mitochondrial DNAs coexisting since the mutation event and lack of complementation of DNAs introduced separately into a cell within distinct organelles. Mol Cell Biol 1994;14:2699–712.
18. Murdock DG, Christacos NC, Wallace DC. The age-related accumulation of a mitochondrial DNA control region mutation in muscle, but not brain, detected by a sensitive PNA-directed PCR clamping based method. Nucleic Acids Res 2000;28:4350–5.
19. Hancock DK, Schwarz FP, Song F, Wong LJ, Levin BC. Design and use of a peptide nucleic acid for detection of the heteroplasmic low-frequency mitochondrial encephalomyopathy, lactic acidosis, and stroke-like episodes (MELAS) mutation in human mitochondrial DNA. Clin Chem 2002;48:2155–63.
20. Ingman M, Kaessmann H, Paabo S, Gyllenstein V. Mitochondrial genome variation and the origin of modern humans. Nature 2000;408:708–13.
21. Finnila S, Lehtonen MS, Majamaa K. Phylogenetic network for European mtDNA. Am J Hum Genet 2001;68:1475–84.
22. Kong QP, Yao YG, Sun C, Bandelt HJ, Zhu CL, Zhang YP. Phylogeny of east Asian mitochondrial DNA lineages inferred from complete sequences. Am J Hum Genet 2003;73:671–6.
23. Herrnstadt C, Elson JL, Fahy E, Preston G, Turnbull DM, Anderson C, et al. Reduced-median-network analysis of complete mitochondrial DNA coding-region sequences for the major African, Asian, and European haplogroups. Am J Hum Genet 2002;70:1152–71.
24. Tanaka M. Human mitochondrial genome polymorphism database. http://www.giib.or.jp/mtsnp/index_e.html (accessed May 2004).
25. Nomiyama T, Tanaka Y, Hattori N, Nishimaki K, Nagasaka K, Kawamori R, et al. Accumulation of somatic mutation in mitochondrial DNA extracted from peripheral blood cells in diabetic patients. Diabetologia 2002;45:1577–83.
26. Suzuki Y, Nishimaki K, Taniyama M, Muramatsu T, Atsumi Y, Matsuoka K, et al. Lipoma and opthalmoplegia in mitochondrial diabetes associated with small heteroplasmy level of 3243 tRNA(Leu(UUR)) mutation. Diabetes Res Clin Pract 2004;63: 225–9.

MOLECULAR AND CELLULAR BIOLOGY, Nov. 2004, p. 9823–9834 Vol. 24, No. 22
0270-7306/04/$08.00+0 DOI: 10.1128/MCB.24.22.9823–9834.2004

Architectural Role of Mitochondrial Transcription Factor A in Maintenance of Human Mitochondrial DNA

Tomotake Kanki,[1] Kippei Ohgaki,[1] Martina Gaspari,[2] Claes M. Gustafsson,[2] Atsushi Fukuoh,[1] Narie Sasaki,[3] Naotaka Hamasaki,[1] and Dongchon Kang[1]*

Department of Clinical Chemistry and Laboratory Medicine, Kyushu University Graduate School of Medical Sciences, Higashi-ku, Fukuoka,[1] and Department of Biology, Faculty of Science, Ochanomizu University, Tokyo,[3] Japan, and Department of Medical Nutrition, Karolinska Institute, Novum, Hudddinge, Sweden[2]

Received 29 December 2003/Returned for modification 17 March 2004/Accepted 26 August 2004

Mitochondrial transcription factor A (TFAM), a transcription factor for mitochondrial DNA (mtDNA) that also possesses the property of nonspecific DNA binding, is essential for maintenance of mtDNA. To clarify the role of TFAM, we repressed the expression of endogenous TFAM in HeLa cells by RNA interference. The amount of TFAM decreased maximally to about 15% of the normal level at day 3 after RNA interference and then recovered gradually. The amount of mtDNA changed closely in parallel with the daily change in TFAM while in organello transcription of mtDNA at day 3 was maintained at about 50% of the normal level. TFAM lacking its C-terminal 25 amino acids (TFAM-ΔC) marginally activated transcription in vitro. When TFAM-ΔC was expressed at levels comparable to those of endogenous TFAM in HeLa cells, mtDNA increased twofold, suggesting that TFAM-ΔC is as competent in maintaining mtDNA as endogenous TFAM under these conditions. The in organello transcription of TFAM-ΔC-expressing cells was no more than that in the control. Thus, the mtDNA amount is finely correlated with the amount of TFAM but not with the transcription level. We discuss an architectural role for TFAM in the maintenance of mtDNA in addition to its role in transcription activation.

Human mitochondrial DNA (mtDNA) is a 16.5-kb double-stranded circular molecule that encodes 13 essential protein components of the mitochondrial oxidative phosphorylation complexes. The maintenance of mtDNA integrity is essential for normal function of the respiratory chain that is responsible for aerobic ATP production. There are hundreds to thousands of copies of mtDNA in one cell. Because the level of mtDNA transcripts largely depends on the copy number of mtDNA, the regulation of its copy number is important for maintaining mitochondrial ATP production. However, the regulation of mtDNA copy number is still poorly understood.

Mitochondrial transcription factor A (TFAM) (11, 30), a transcription factor for mtDNA, enhances mtDNA transcription in a promoter-specific fashion in the presence of mitochondrial RNA polymerase and transcription factor B (TFB1 M or TFB2 M) (10, 23). TFAM is a member of the high-mobility group (HMG) proteins because it contains two HMG boxes. TFAM possesses DNA-binding properties regardless of sequence specificity, although it shows a higher affinity for the light- and heavy-strand promoters (LSP and HSP, respectively) (11, 30). In addition to these two HMG boxes, human TFAM has a linker region between the two HMG boxes and a carboxyl-terminal tail region (C-tail) composed of 27 and 25 residues, respectively (6).

* Corresponding author. Mailing address: Department of Clinical Chemistry and Laboratory Medicine, Kyushu University Graduate School of Medical Sciences, 3-1-1 Maidashi, Higashi-ku, Fukuoka 812-8582, Japan. Phone: 81-92-642-5749. Fax: 81-92-642-5772. E-mail: kang@mailserver.med.kyushu-u.ac.jp.

According to the strand-coupled model (4, 16, 38), replication of the L-strand, i.e., lagging-strand replication, occurs simultaneously with that of the H-strand. On the other hand, in another mtDNA replication model, the strand displacement model (34), replication of the nascent H-strand proceeds and displaces the parental H-strand until a replication origin of the L-strand, O_L, is exposed on a single strand. The process of mtDNA replication begins with the initiation of transcription at LSP. The transcript initiated from LSP forms an RNA-DNA hybrid at a replication origin for the H-strand, O_H. The RNA-DNA hybrid is processed to generate an RNA primer utilized by mitochondrial DNA polymerase γ (20). Thus, in the latter model, the replication of mammalian mtDNA is proposed to be coupled with transcription, and therefore TFAM is thought to be essential for replication of mtDNA (34). The role of transcription in the former model has not yet been clarified.

Abf2p, a TFAM homolog in *Saccharomyces cerevisiae*, has two HMG boxes and a short linker region between them, but unlike TFAM, it does not have a C-tail (12). Abf2p is abundant in mitochondria, with one Abf2p polypeptide present for every 15 bp of mtDNA (8). Disruption of the ABF2 gene leads to a loss of mtDNA and a resultant loss of respiratory competence when cells are grown in the presence of glucose. Expression of human TFAM in the *S. cerevisiae abf2* strain rescued the phenotype, implying a potential functional homology between human TFAM and Abf2p (30). However, unlike mammalian TFAM, Abf2p is not required for the initiation of transcription in yeast mtDNA (8). An in vitro transcription assay demonstrated that Abf2p or C-tail-deleted TFAM does not activate transcription, whereas a chimeric Abf2p containing the C-tail

does (6), suggesting that the C-tail of TFAM is necessary for transcriptional activation. This notion is also supported by a recent report that the C-tail of TFAM is necessary to bind mitochondrial transcription factor B (TFBM) and that this binding is required for transcription activation (24). In agreement with this, the import of full-length TFAM into isolated mitochondria increases transcription, but import of TFAM lacking the C-tail does not (14). Thus, the C-tail of TFAM is considered essential for the activation of transcription.

The mitochondrial nucleoids, protein-mtDNA complexes, have been studied extensively in the lower eukaryotes *S. cerevisiae* (17, 26) and *Physarum polycephalum* (32). In *S. cerevisiae* Abf2p is detected as a main component of the nucleoid and appears to function to maintain mtDNA and the nucleoid structure (17). In *P. polycephalum*, Glom, which also has two HMG boxes, shows a strong DNA-packaging activity (32). Both of these HMG family proteins can be functionally replaced by an *Escherichia coli* histone-like protein, HU (25, 32), implying that Abf2p and Glom package mtDNA.

There are several reports that mtDNA in higher eukaryotes is somewhat naked except for the D-loop region (2, 7, 29, 31), while the mtDNA of *Xenopus laevis* is reported to be packaged into regular beaded structures (3). These conflicting results on whether animal mtDNA takes on a higher nucleosome- or chromatin-like structure (mitochondrial nucleoid or mitochromatin/mitochondrial chromosome) are not fully resolved. Recent reports also suggest the existence of such a higher mtDNA structure in mammals (1, 13, 35). Because the amount of human TFAM is sufficient to cover the entire region of mtDNA (36) and because most TFAM molecules indeed bind to mtDNA (1), TFAM has been proposed to be one of the main components of the human mtDNA higher structure.

Homozygous gene disruption of *Tfam* is lethal in both mouse and chicken cells, at least in part due to mtDNA depletion and resultant loss of oxidative phosphorylation capacity (19, 22). In heterozygous cells, the expression of mouse and chicken TFAM was reduced by about 50% and the amount of mtDNA also decreased by about half (19, 22). These results suggest that TFAM is necessary to maintain mtDNA. There are two possibilities to explain mtDNA maintenance by TFAM. One is that, given that the replication of mtDNA is coupled to transcription (34), TFAM affects the replication of mtDNA directly. The other is that TFAM binds and stabilizes mtDNA, as do other HMG family proteins (5, 8, 12, 32, 39).

There have been no reports demonstrating overexpression of TFAM in mammalian cells. We established stable and inducible human cell lines overexpressing TFAM for the first time with a tetracycline-regulated gene expression system. In this study, with these TFAM-overexpressing cell lines and RNA interference (RNAi), we manipulated the amount of human TFAM in human HeLa cell lines and then analyzed mtDNA and mitochondrial transcription. We found that the amount of TFAM but not the transcription level is correlated to the amount of mtDNA.

MATERIALS AND METHODS

Antibodies. Antibodies to human TFAM, prohibitin, and BAP37 were produced by immunizing rabbits with recombinant glutathione *S*-transferase–human TFAM (28), glutathione *S*-transferase–prohibitin, and glutathione *S*-transferase–BAP37 proteins, respectively. Antibodies to cytochrome *b* and complex II were produced by immunizing rabbits with peptides of the C-terminal eight amino acids of cytochrome *b* and the C-terminal nine amino acids of the complex II iron sulfur protein, respectively (1). An antibody to human mitochondrial single-stranded DNA-binding protein (mtSSB) was described previously (36) as was an antibody to P32 (27). Antibodies against the hemagglutinin (HA) HA.11 epitope tag, cytochrome *c*, and calnexin were obtained from Covance, Stressgen, and Santa Cruz Biotechnology, respectively.

Preparation of tetracycline-regulated TFAM-overexpressing cell lines. To avoid suppression by RNAi, we introduced silent mutations in a human TFAM cDNA corresponding to the RNAi target in advance (from GTCTTGGCAAGT TGTCCAAAGAAACCTGTAAGTTCT to GTCTTAGCAAGTTGCCCTA AAAAGCCTGTAAGCTCT; the encoded amino acid sequence for both is VLASCPKKPVSS [amino acids 45 to 56]; sites where silent mutations have been introduced are in boldface) and named it pmod-TFAM. A DNA fragment encoding human TFAM lacking the C-terminal 25 amino acids (human TFAM-ΔC), i.e., it retained amino acids 1 to 221, was amplified with pMod-TFAM as a template. The sense primer contained a BamHI site, the Kozak sequence (18), and ATG for a first methionine in that order; the antisense primer contained an SpeI site. A DNA fragment specifying an HA tag was prepared by annealing the complementary synthesized oligonucleotides, which included, in order, the sequences for an SpeI restriction site, an HA epitope tag (11 amino acids), a stop codon, and an NheI site.

The DNA fragments for human TFAM and the HA tag were digested with appropriate restriction enzymes and inserted between the BamHI and NheI sites of vector pTRE2hyg (Clontech). This vector encodes the precursor human TFAM-ΔC with the HA tag at its C terminus and was named ph-TFAM-ΔC-HA. We also amplified a DNA fragment encoding precursor mouse TFAM (amino acids 1 to 243) by PCR, with a mouse cDNA library as a template with a sense primer (containing, in order, a BamHI site, the Kozak sequence [18], and ATG for a first methionine) and an antisense primer (containing an SpeI site). The mouse TFAM DNA fragment and the HA tag DNA fragment were inserted into the pTRE2hyg vector in the same way as the human construct (pm-TFAM-HA).

A HeLa Tet-Off cell line was obtained from Clontech. The cells were grown in Dulbecco's modified Eagle's medium (DMEM) with 10% fetal bovine serum (Gibco) and 100 μg of G418 per ml (Sigma). We transfected HeLa Tet-Off cells with our plasmids with the FuGene 6 reagent (Roche Molecular Biochemicals) and selected cells bearing the transgenes in the presence of G418 (400 μg/ml) (Wako), hygromycin B (200 μg/ml) (Wako), and doxycycline, a tetracycline derivative (1 μg/ml) (ICN Biomedicals). We isolated hygromycin-resistant clones, cultured them with or without doxycycline for about 10 days, and then examined the expression of recombinant proteins by Western blotting. These mouse and human TFAM-overexpressing cell lines were designated MTF (mouse TFAM full-length) and HΔC (human C-tail-deleted TFAM), respectively.

Suppression of human TFAM by RNAi. HeLa cells were grown in DMEM with 10% fetal bovine serum and antibiotics (100 μg of G418 per ml for control HeLa Tet-Off cells; 100 μg of G418 and 100 μg of hygromycin B per ml for MTF and HΔC cells) in 3.5-cm dishes. When the cells were about 50% confluent, the culture medium was replaced by 2 ml of DMEM containing 10% fetal bovine serum with and without doxycycline (1 μg/ml). The sequences of short interfering RNA (siRNA) duplexes were 5′-GUUGUCCAAAGAAACCUGUdTdT-3′ (sense siRNA) and 5′-ACAGGUUUCUUUGGACAACdTdT-3′ (antisense siRNA) (obtained from Qiagen); 12 μl of 20 μM siRNA duplexes was mixed with 200 μl of Opti-MEM (Gibco) in one tube; 12 μl of Oligofectamine (Invitrogen) was mixed with 48 μl of Opti-MEM in the other tube. The two mixtures were incubated for 10 min at room temperature and then combined and mixed gently by pipetting. The combined mixture was allowed to stand for another 20 min at room temperature. The siRNA-Oligofectamine mixture was then added to the cultured cells. After 24 h, the culture medium was replaced by new DMEM with 10% fetal bovine serum and appropriate antibiotics. When the cells were almost confluent, they were reseeded in two 3.5-cm dishes.

Western blotting. The cells from a 3.5-cm dish were collected in 1 ml of phosphate-buffered saline (PBS), and half of them were solubilized with 100 μl of sodium dodecyl sulfate (SDS) denaturing buffer consisting of 0.5% SDS and 1% 2-mercaptoethanol (the other half was used for mtDNA quantification [see below]). The mixture was briefly sonicated immediately after solubilization. Proteins were separated on an SDS–12% polyacrylamide gel by polyacrylamide gel electrophoresis (PAGE) and subsequently detected by immunoblotting. The signals were visualized with horseradish peroxidase-labeled anti-rabbit immunoglobulin G (Biosource) and ECL reagents (Amersham Biosciences). The chemiluminescence was recorded and quantified with a chilled charge-coupled device camera, LAS1000plus (Fuji).

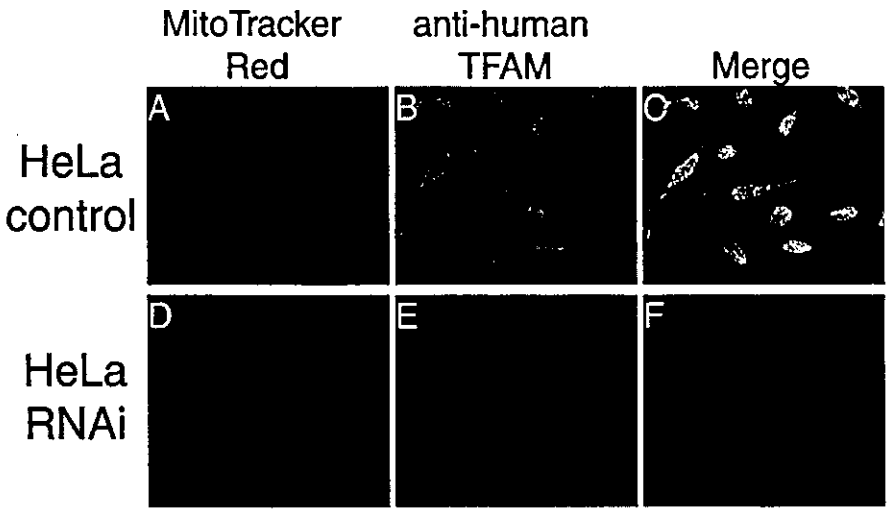

FIG. 1. Immunofluorescent images of HeLa cells treated by RNAi. Human TFAM in HeLa cells was identified with anti-human TFAM antibodies (B and E). Mitochondria were stained with MitoTracker Red (A and D). Panels C and F are merged images of panels A plus B and D plus E, respectively.

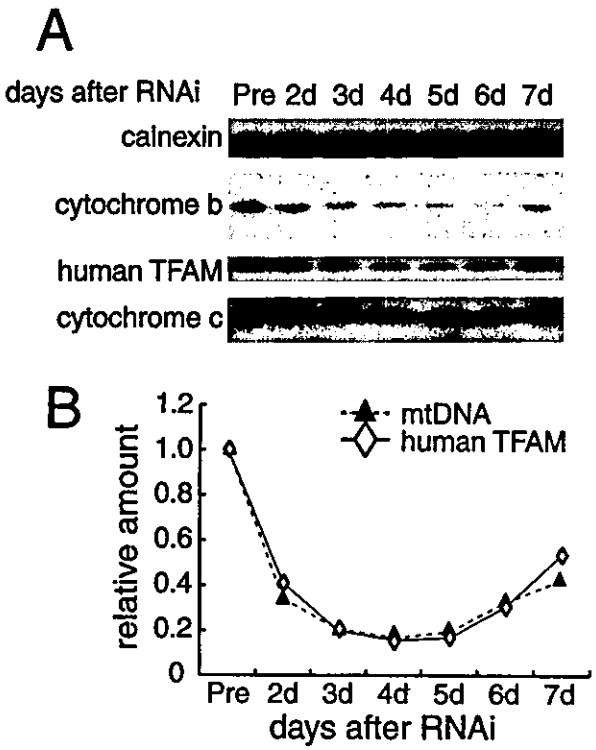

FIG. 2. Parallel decreases and increases in human TFAM and mtDNA after RNAi. (A) Calnexin (as a standard of cell amount), cytochrome *b*, human TFAM, and cytochrome *c* in HeLa cells were analyzed by Western blotting 2 to 7 days after RNAi. The relative amount of mtDNA was measured by quantitative PCR. (B) Representative daily changes in the relative amounts of human TFAM (◇) and mtDNA (▲).

Quantification of mtDNA. From the remaining half of the cells, total DNA was extracted with a DNeasy tissue kit (Qiagen). The total DNA was quantified with a PicoGreen double-stranded DNA quantitation kit (Molecular Probes). The relative amount of mtDNA was quantified by quantitative PCR with a LightCycler (Roche). The PCR mixture contained 2 ng of the total DNA (for a standard curve, 8, 4, 2, 1, and 0.5 ng of the total DNA were used), 10 pmol each of primers (5′-CCACCCAAGTATTGACTCACCC-3′ [nucleotides 16052 to 16073] and 5′-CGAGAAGGGATTTGACTGTAATG-3′ [nucleotides 16339 to 16361]) and 3 mM $MgCl_2$ in 20 μl. To estimate the amount of genomic DNA as an internal standard, a genomic beta-globin gene was amplified in a 20-μl reaction mixture containing 16 ng of the total DNA (for a standard curve, 64, 32, 16, 8, and 4 ng of the total DNA were used), 10 pmol each of primers (5′-CTGCCCTGTGGG GCAAGGTGAACGTGGATG-3′ and 5′-CAGGTGAGCCAGGCCATCACT AAAGGCACC-3′), and 3 mM $MgCl_2$. The amount of mtDNA was adjusted to the amount of genomic DNA.

Immunofluorescent imaging of HeLa cells. Cells were incubated in the presence of 100 nM MitoTracker Red CMXRos (Molecular Probes) for 20 min. After washing with PBS three times, the cells were fixed with acetone-methanol (50:50, vol/vol) for 5 min. After washing with PBS three times, the fixed cells were blocked with bovine serum albumin-PBS (1% bovine serum albumin in PBS) for 30 min, then incubated with 250-fold-diluted anti-human TFAM antiserum or anti-HA antibody in bovine serum albumin-PBS for 1 h. After washing the cells with wash buffer (0.1% Tween 20 in PBS) three times, cells were incubated with 250-fold-diluted Alexa Fluor 488 goat anti-rabbit immunoglobulin G (Molecular Probes) for 30 min. Fluorescence images were taken with a confocal laser microscope (Bio-Rad Laboratories).

Isolation of mitochondria from HeLa cells. All procedures were done at 4°C. HeLa cells cultured in 10-cm dishes were scraped with a cell lifter (Costar) into 3 ml of PBS, pelleted by centrifugation, and washed with homogenization buffer (10 mM HEPES-KOH, pH 7.4, and 0.25 M sucrose). The cells were suspended in 4 volumes of the buffer and homogenized with a Potter-Elvehjem homogenizer. The homogenate was centrifuged at 900 × *g* for 10 min to remove the unbroken cells and nuclei. The supernatant was centrifuged at 10,000 × *g* for 6 min. The pellet was collected as a crude mitochondrial fraction and used for in organello transcription assays or for preparing Nonidet P-40-insoluble fractions.

In vitro transcription assay. The cDNA coding for mature human TFAM (amino acid residues 42 to 246) and mature human TFAM-ΔC-HA (amino acid residues 42 to 221 and C-terminal HA tag) were inserted into the pProEXHTb vector (Gibco). The recombinant His-human TFAM and His-human TFAM-ΔC-HA were expressed in *Escherichia coli* BL21 cells and purified Ni^{2+}-bound chelating Sepharose resin (Amersham Biosciences) as described previously (28, 36). In vitro transcription reactions were performed with a cloned DNA fragments corresponding to nucleotides 1 to 477 of human mtDNA as previously described (10).

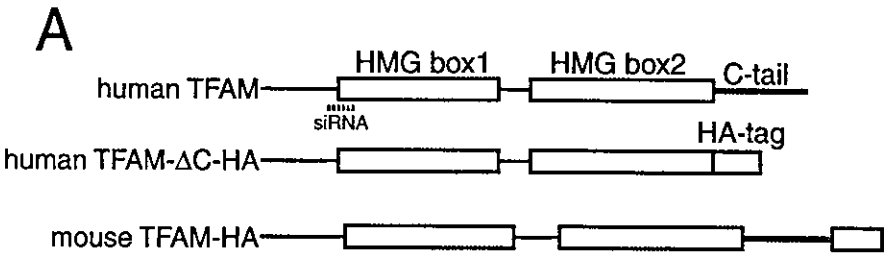
A
HMG box1
HMG box2
C-tail
human TFAM
siRNA
HA-tag
human TFAM-ΔC-HA
mouse TFAM-HA

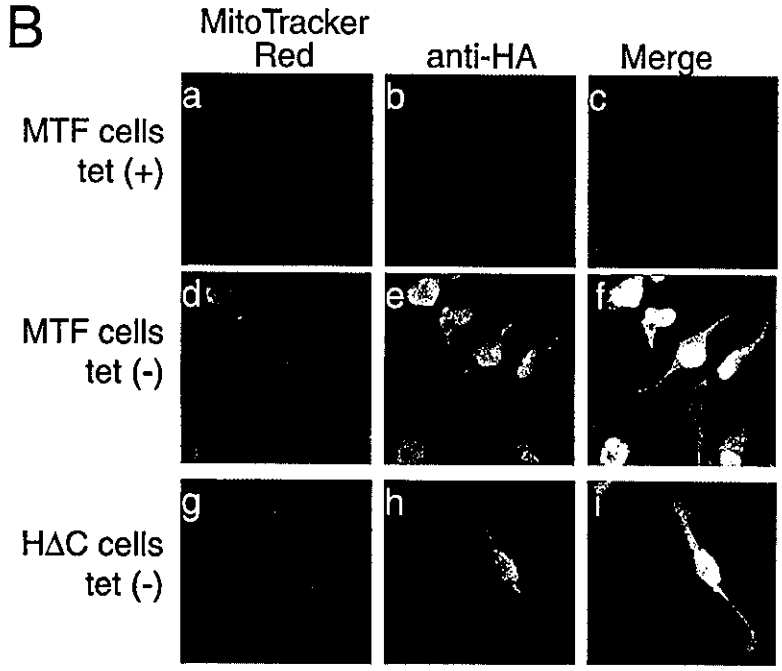
B
MitoTracker Red
anti-HA
Merge
MTF cells tet (+)
MTF cells tet (-)
HΔC cells tet (-)
a
b
c
d
e
f
g
h
i

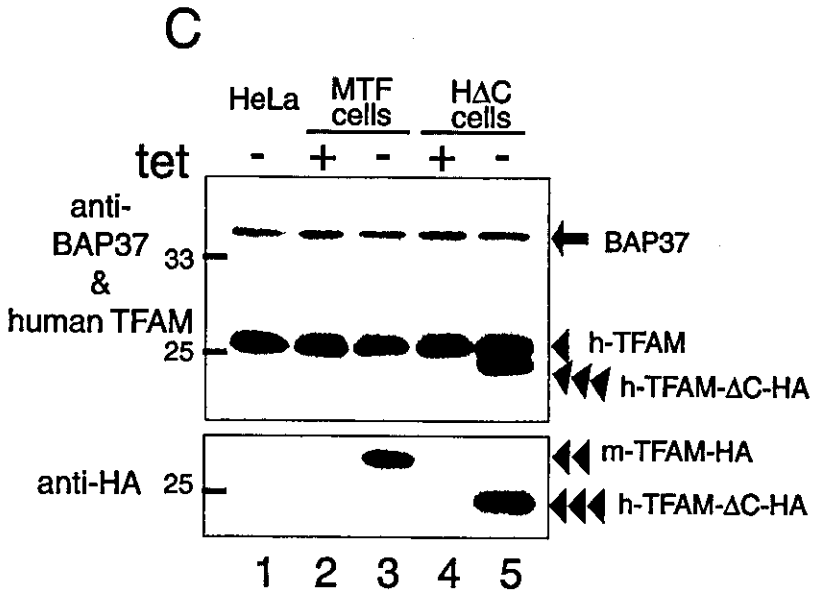
C
HeLa
MTF cells
HΔC cells
tet - + - + -
anti-BAP37 & human TFAM
33
25
BAP37
h-TFAM
h-TFAM-ΔC-HA
anti-HA
25
m-TFAM-HA
h-TFAM-ΔC-HA
1 2 3 4 5

In organello transcription assay. In organello transcription was measured by the method of Enriquez et al. with slight modifications (9). The mitochondrial fraction was resuspended in transcription buffer (10 mM Tris-HCl [pH 7.4], 25 mM sucrose, 75 mM sorbitol, 100 mM KCl, 10 mM K_2HPO_4, 50 μM EDTA, 5 mM $MgCl_2$, 1 mM ATP, 1 mg of bovine serum albumin per ml). Mitochondria (200 μg of protein) were incubated in 300 μl of the transcription buffer containing 10 μCi of [α-^{32}P]UTP (Amersham Biosciences) at 37°C for 30 min. After the incubation, the mitochondria were pelleted at 15,000 × *g* for 1 min and then washed with nuclease buffer (0.25 M sucrose, 10 mM Tris-HCl [pH 8.0], 1 mM $CaCl_2$). The mitochondria were resuspended in 400 μl of nuclease buffer with 100 units of nuclease S7 (Roche Molecular Biochemicals) and incubated at room temperature for 20 min. The mitochondria were then pelleted at 15,000 × *g* for 1 min and washed with TES buffer (10 mM Tris-HCl [pH 7.4], 1 mM EDTA, 0.25 M sucrose). The mitochondrial pellet was solubilized in 100 μl of lysis buffer (50 mM Tris-HCl [pH 8.0], 20 mM NaCl, 1 mM EDTA, 1% SDS) containing 20 μg of protease K (Gibco) and incubated at room temperature for 15 min. After addition of 100 μl of a phenol-chloroform-isoamyl alcohol mixture (25:25:1, vol/vol/vol) and vortexing for 1 min, the mixture was centrifuged at 20,000 × *g* for 5 min, and 80 μl of the aqueous phase was transferred to a clean tube. Then 1 μl of Pellet Paint (Novagen), 80 μl of 3 M sodium acetate (pH 5.2), and 300 μl of ethanol were added, and the mitochondrial nucleic acids were precipitated. The pellets were solubilized with sample buffer (99% formamide, 1 mM EDTA, and bromphenol blue) and incubated at 95°C for 3 min. DNA size makers (100-bp DNA ladder and 1-kb DNA ladder, New England BioLabs) were [γ-^{32}P]ATP labeled with Ready-To-Go T4 polynucleotide kinase (Amersham Biosciences). Samples were separated on an 8 M urea–4% polyacrylamide gel by electrophoresis and analyzed with a BAS-2500 (Fuji). The isolated mitochondria (5 μg) were analyzed by Western blotting to check the amount of mitochondria and efficiency of RNAi.

Separation of mitochondrial NP-40-soluble and -insoluble fractions. The mitochondria were resuspended in TES buffer containing 0.5% NP-40 and 1 mM dithiothreitol (0.5 mg of protein/ml) and incubated for 30 min on ice with intermittent mixing. The mitochondria were centrifuged at 20,000 × *g* for 30 min and separated into a pellet (P1) and a supernatant (S1). The P1 fraction (10 μg of protein) was resuspended with 20 μl of nuclease buffer (10 mM Tris-HCl [pH 7.4], 0.25 M sucrose, 1 mM dithiothreitol, 2.5 mM $CaCl_2$, and 0.5% NP-40) and incubated for 30 min on ice with 2.5 U of nuclease S7 or 0.5 μg of RNase A (DNase free; Wako). After centrifugation at 20,000 × *g* for 30 min, the sample was separated into a pellet (P2) and a supernatant (S2). Proteins from each fraction were separated by SDS-PAGE and subsequently analyzed by Western blotting with appropriate primary antibodies.

mtDNA in the P1 and S1 fractions was detected by PCR as described previously (1). Briefly, total mitochondria, P1, and S1 (from 10 μg of mitochondria) were incubated at 95°C for 30 min with 0.5 μg of protease K (Gibco) and diluted in 200 μl of distilled water. With 1 μl each of the diluted samples, a fragment of mtDNA was amplified with PCR primers (nucleotides 16052 to 16073 and nucleotides 16339 to 16361) and Ex-taq DNA polymerase (Takara). The number of amplification cycles was 25, and the PCR products were separated on a 1% agarose gel.

RESULTS

Reduced expression of human TFAM by RNAi. To observe a dose effect of TFAM, we downregulated the expression of human TFAM by RNAi in HeLa cells. Three days after RNAi treatment, human TFAM was barely detectable on immunofluorescent images with anti-human TFAM antibodies (compare Fig. 1B and E). To monitor the change in the levels of human TFAM and other mitochondrial proteins, cells were collected daily between days 2 and 7 and analyzed by Western blotting (Fig. 2A). The amount of human TFAM was decreased maximally at days 3 and 4 and then gradually increased again (Fig. 2A, third panel). The amounts of calnexin, a microsomal protein, and cytochrome *c*, a nucleus-encoded mitochondrial protein, did not change (Fig. 2A, top and bottom panels). The amounts of several other nucleus-encoded mitochondrial proteins (prohibitin, BAP37, and VDAC) were not affected by this RNAi (data not shown), confirming the specificity of the RNAi treatment. The reduction in cytochrome *b*, an mtDNA-encoded protein (Fig. 2A, second panel), probably resulted from a decrease in mtDNA (Fig. 2B). We measured the relative amount of mtDNA by quantitative PCR and found that the amount fell and rose in parallel with that of human TFAM (Fig. 2B). The levels of human TFAM and mtDNA were 0.141 ± 0.052 and 0.132 ± 0.061 (n = 4) of those of control cells at day 3. Thus, the amount of mtDNA was strongly correlated with the amount of TFAM in vivo.

Preparation of tetracycline-regulated TFAM-overexpressing cell lines. Conversely, to see whether an increase in TFAM would affect the amount of mtDNA, we created TFAM-overexpressing cell lines. We made two kinds of Tet-Off gene expression vectors, ph-TFAM-ΔC-HA and pm-TFAM-HA, in order to express C-tail-deleted human TFAM with an HA tag and mouse full-length TFAM with an HA tag, respectively (Fig. 3A). To produce the stable TFAM-expressing cell lines, we transfected HeLa Tet-Off cells with each vector and cultured them with hygromycin for selection and with doxycycline to suppress expression. We isolated hygromycin-resistant colonies and checked the expression of TFAM by Western blotting after culturing for 10 days without doxycycline. Fourteen of 24 hygromycin-resistant ph-TFAM-ΔC-HA-transfected clones expressed high levels of human TFAM-ΔC-HA (about 50 to 120% compared with the amount of endogenous human TFAM). Thirteen of 24 hygromycin-resistant pm-TFAM-HA-transfected clones expressed high levels of mouse TFAM-HA (about 50 to 140% compared with the amount of endogenous human TFAM). These mouse TFAM- and human TFAM-ΔC-overexpressing cell lines were designated MTF (mouse TFAM full-length) and HΔC (human C-tail-deleted TFAM), respectively.

When cultured without doxycycline, immunofluorescent imaging of MTF cells with anti-HA antibodies showed granular fluorescence. This pattern colocalized with that of MitoTracker Red, a mitochondrion-staining fluorescent dye (Fig. 3B, panels d to f), indicating that the expressed exogenous TFAM localized to mitochondria, while the cells cultured with doxycycline showed almost no fluorescence with anti-HA an-

FIG. 3. Tetracycline-regulated expression of TFAM. (A) The scheme of recombinant TFAM molecules. Human and mouse TFAM have two HMG boxes (white square) and a C-tail region (gray bar). An HA.11 epitope tag is indicated by a gray square. The position of the RNAi target is indicated by a dotted line. (B) MTF cells and HΔC cells were cultured with doxycycline [tet (+)] or without doxycycline [tet (−)]. Mitochondria were stained with MitoTracker Red (panels a, d, and g), and recombinant TFAM was stained with anti-HA antibodies (panels b, e, and h). The merged images are shown in panels c, f, and i. (C) Western blotting analysis of TFAM molecules. Total cell lysates were used for Western blotting. BAP37 (arrow) is shown as an internal standard for the amount of protein applied in the samples. Antibodies for BAP-37 and human TFAM were added together for detecting the two proteins (upper panel). Then the membrane was reprobed with anti-HA antibody (lower panel). Endogenous human TFAM (arrowhead), exogenous mouse TFAM-HA (double arrowheads), and exogenous human TFAM-ΔC-HA (triple arrowheads) are indicated.

tibodies (Fig. 3B, panel b). HΔC cells showed the same pattern as the MTF cells (Fig. 3B, panels g to i). With Western blots, mouse TFAM-HA was detected by anti-HA antibodies in medium without doxycycline (double arrowheads), whereas there was no signal in medium containing doxycycline (Fig. 3C, compare lanes 2 and 3 in the lower panel). Anti-human TFAM did not react with mouse TFAM (Fig. 3C, lane 3; notice their molecular sizes). Similarly, human TFAM-ΔC-HA (triple arrowheads) was detected by both anti-human TFAM and anti-HA antibodies only in medium without doxycycline (Fig. 3C, lanes 4 and 5 in the upper and lower panels). Thus, expression of the recombinant proteins was completely regulated by doxycycline. Endogenous human TFAM (single arrowhead) was not affected by the overexpression of exogenous TFAM (Fig. 3C, upper panel). The amount of BAP37 (arrow), an inner membrane protein, was not altered (Fig. 3C, upper panel), indicating that the amount applied was essentially the same among all samples.

Overexpression of mouse TFAM-HA or human TFAM-ΔC-HA increases the amount of mtDNA. Because it takes about 10 days to stably express exogenous mouse TFAM-HA or human TFAM-ΔC-HA after removal of doxycycline (data not shown), we did experiments at least 14 days after removal of doxycycline. In medium without doxycycline, the amounts of mouse TFAM-HA and human TFAM-ΔC-HA were 0.77 ± 0.17 (mean ± standard deviation) and 1.05 ± 0.11, respectively, of that of endogenous human TFAM; i.e., the total amount of TFAM was 1.77 and 2.05, respectively, that of cells grown in medium with doxycycline (Fig. 4B). Overexpression of total TFAM by a factor of 1.77 (in MTF cells) and 2.05 (in HΔC cells) increased the amount of mtDNA by a factor of 1.89 ± 0.22 and 1.99 ± 0.18, respectively (Fig. 4B). Neither nucleus-encoded mitochondrial proteins (prohibitin and cytochrome *c*) nor an mtDNA-encoded protein, cytochrome *b*, was affected by the overexpression of TFAM (Fig. 4A). Thus, the amount of TFAM led the change in mtDNA levels in parallel.

Both mouse TFAM-HA and human TFAM-ΔC-HA can maintain the amount of mtDNA. mtDNA was increased by the overexpression of C-tail-deleted human TFAM, which is considered not to activate transcription (6), raising the possibility that the increase in mtDNA does not require the upregulation of transcription. In order to clarify this point, we performed RNAi in the TFAM-overexpressing cells. To avoid suppression of recombinant human TFAM by the RNAi treatment, silent mutations were introduced into a cDNA of human TFAM (see Methods). In medium with doxycycline, MTF cells and HΔC cells expressed little or no mouse TFAM-HA (Fig. 5A, double arrowheads; lanes 1 and 2) and human TFAM-ΔC-HA (Fig. 5A, triple arrowheads; lanes 5 and 6), respectively. However, In medium without doxycycline, the exogenous TFAM proteins were overexpressed (Fig. 5A, bottom panel, lanes 3, 4, 7, and 8). The RNAi treatment (i.e., 3 days after RNAi) suppressed the endogenous TFAM (Fig. 5A, fourth panel, lanes 2, 4, 6, and 8), but exogenous TFAMs were not affected (Fig. 5A, bottom panel, lanes 4 and 8; double and triple arrowheads), showing selective downregulation of endogenous human TFAM.

In MTF cells in which mouse TFAM is not yet expressed but endogenous TFAM is repressed by RNAi (Fig. 5B), mtDNA was reduced compared to that in the MTF cells in which

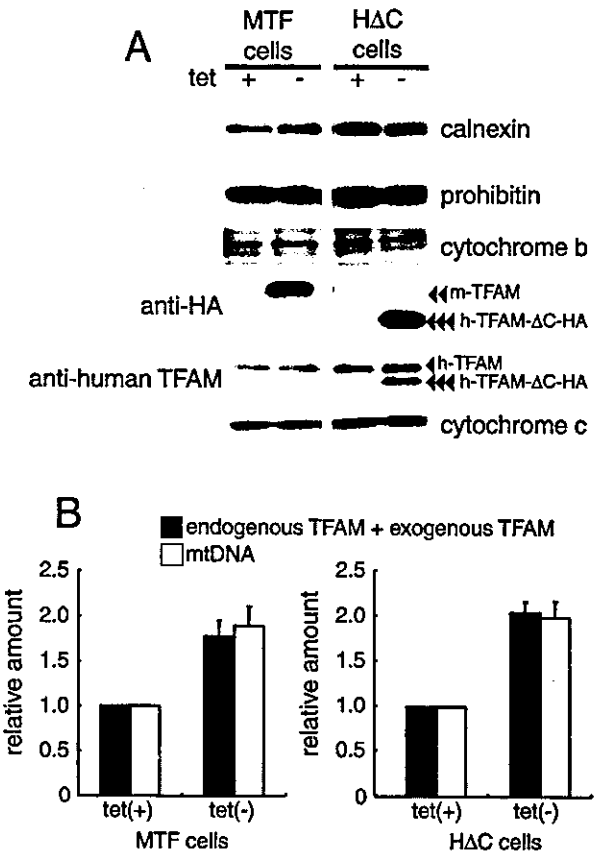

FIG. 4. Amount of mitochondrial proteins and mtDNA in MTF and HΔC cells. (A) Total cell lysates of cells cultured with doxycycline [tet (+)] or without doxycycline [tet (−)] were used for Western blotting. Prohibitin and cytochrome *c* are mitochondrial proteins encoded by the nuclear genome. Cytochrome *b* is a mitochondrial protein encoded by mtDNA. Endogenous human TFAM (arrowhead), mouse TFAM-HA (double arrowheads), and human TFAM-ΔC-HA (triple arrowheads) are indicated. Calnexin, a microsomal protein, is shown as an internal standard. (B) Quantification of relative amounts of TFAM (black bar) and mtDNA (gray bar). Signal intensities on the Western blots were measured for estimating the number of TFAM molecules, endogenous TFAM, and exogenous TFAM. The amount of mtDNA was measured by quantitative PCR. Error bars indicate ±1 standard deviation from the mean of three independent experiments.

endogenous TFAM is not repressed (Fig. 5B). In MTF cells in which mouse TFAM is expressed but endogenous TFAM is not repressed (Fig. 5B), mtDNA was almost doubled with the twofold increase in total TFAM. mtDNA was reduced to the control level by the RNAi treatment in the mouse TFAM-expressing cells (Fig. 5B). The reduced amount of mtDNA by RNAi in medium without doxycycline roughly equaled that in medium with doxycycline (compare the difference between RNAi with and without doxycycline) (Fig. 5B). A similar pattern was observed in HΔC cells (Fig. 5C). These results suggest that both exogenous TFAMs are as competent in the maintenance of mtDNA as endogenous human TFAM under conditions in which endogenous human TFAM remains at about 15% of the control level.

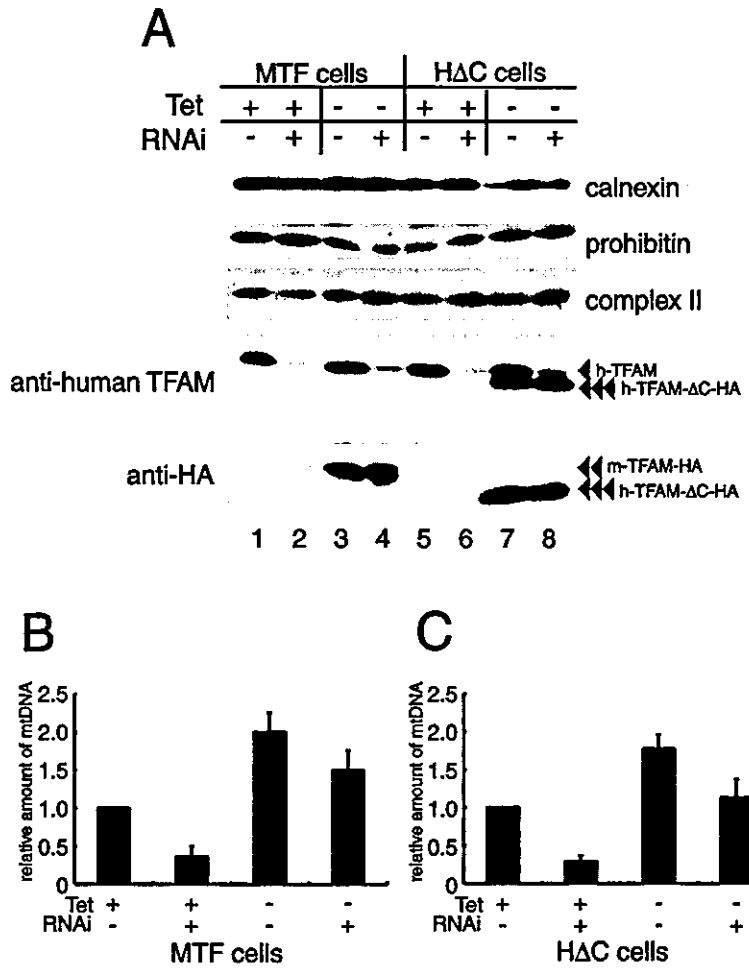

FIG. 5. (A) MTF and HΔC cells were cultured with doxycycline [tet (+)] or without doxycycline [tet (−)]. Three days after RNAi treatment (RNAi +) or without RNAi treatment (RNAi −), the cells were collected and analyzed. The expression of proteins in MTF and HΔC cells was analyzed by Western blotting. Endogenous human TFAM (arrowhead), exogenous mouse TFAM-HA (double arrowheads), and exogenous human TFAM-ΔC-HA (triple arrowheads) are indicated. (B and C) The amount of mtDNA was measured in cells with and without doxycycline and RNAi treatments, as indicated. Error bars indicate ± 1 standard deviation from the mean of three independent experiments.

In vitro and in organello transcription. The C-tail of TFAM is considered essential for initiation of transcription from LSP (6). To confirm that the HA tag does not function like the C-tail, we performed an in vitro transcription assay for human LSP. Human TFAM-ΔC without an HA tag was about 100-fold less active than full-length human TFAM (unpublished data). As expected, a transcript from LSP in the presence of His-human TFAM-ΔC-HA was about 100-fold less than that in the presence of His-human TFAM (Fig. 6A), indicating that LSP-dependent transcription is not increased by adding the HA tag to human TFAM-ΔC.

With the isolated mitochondria from HΔC cells cultured with and without doxycycline and with and without RNAi treatment, we measured transcription in organello by measuring newly synthesized transcripts. The newly synthesized transcripts were labeled with [^{32}P]UTP for 30 min in mitochondria and analyzed by urea-polyacrylamide gel electrophoresis (Fig. 6B). The transcripts were not detected in mitochondria from Rho^0 206 cells (data not shown), excluding any background contribution from genomic transcription. Between the 3,000- and 700-base size markers, the signals for transcription were seen as bands, although the bands were not identified (right panel). In addition to these bands, a smearing background was seen. When human TFAM-ΔC-HA was overexpressed, this smearing background was about 1.6-fold higher (left panel, lane 3) than in the control (lane 1). This nonspecific background was reduced by RNAi treatment (lane 2; by about 60%) and returned to the control level with expression of human TFAM-ΔC-HA (lane 4). The level of the nonspecific smear appeared to be correlated with the amount of mtDNA. The background might reflect nonspecific LSP/HSP-independent transcription or highly heterogeneous RNA processing of LSP/HSP-specific transcription. Another possibility may be RNA primers remaining in nascent mtDNA strands that initiated at diverse sites according to the strand-coupled replication model.

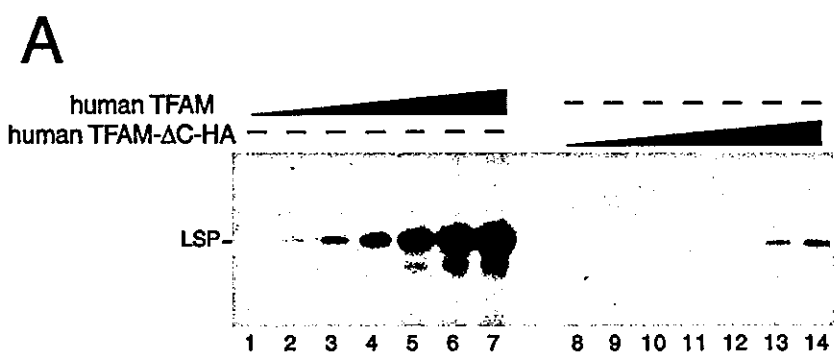

FIG. 6. In vitro and in organello transcription assays. (A) TFAM lacking its C-terminal tail only supports low levels of transcription from LSP. A template containing the light-strand promoter (LSP, 85 fmol) of human mtDNA was used for in vitro runoff transcription assays. The reactions were performed with the following pure recombinant proteins: human mitochondrial RNA polymerase (250 fmol), human TFB2 M (500 fmol), and wild-type human TFAM with an N-terminal His tag or human ΔC-tail TFAM with an N-terminal His tag and C-terminal HA tag (human TFAM-ΔC-HA) in increasing amounts (0.02, 0.05, 0.2, 0.5, 1.6, 5, and 15 pmol). (B) A representative image of five independent experiments is shown. The HΔC cells were cultured with and without doxycycline and treated or not by RNAi, and mitochondria were isolated from these cells 3 days after RNAi treatment. The newly synthesized transcripts were labeled with [α-^{32}P]UTP for 30 min in mitochondria and analyzed by urea-polyacrylamide gel electrophoresis. The approximate size of nucleotides is shown based on the [γ-^{32}P]ATP-labeled DNA size markers (left panel). The part showing bands larger than 600 bases was enlarged (right upper panel). The asterisks indicate measured bands used for estimation. The isolated mitochondria (5 μg of protein) were analyzed by Western blotting to check the protein amount (anti-BAP37 antibody, right lower panel) and the efficiency of RNAi (anti-human TFAM antibody, right middle panel).

Because processed transcripts of mtDNA are distributed mainly between bases 2000 and 700 according to their expected lengths, we hypothesized that the bands found between bases 2000 and 700 are promoter-dependent transcripts (bands marked by asterisks, right panel). The signal intensities were corrected by subtracting the background. When human TFAM-ΔC-HA was overexpressed (lane 3), the specific signals were not changed or somewhat decreased (61 to 113%; average, 77%) in spite of the twofold increase in the amount of mtDNA. This inhibition may be caused by competition between TFAM-ΔC-HA and endogenous TFAM for the promoters. When wild-type human TFAM was reduced by RNAi, the specific signals were reduced to about 46% (41 to 53%) and 49% (44 to 74%) of the control in control and human TFAM-ΔC-HA-overexpressing cells, respectively (lanes 2 and 4), while the amount of mtDNA was about 0.2 and 1 times that of the control cells, respectively (Fig. 5C). Compensatory upregulation of the transcription seems to occur in the former situation. The decrease in the latter may also be due to the competition. Thus, the amount of mtDNA was not correlated with the transcription level.

Both mouse TFAM-HA and TFAM-ΔC-HA are components of the mitochondrial nucleoid. We have previously demonstrated that mtDNA and human TFAM were mostly included in the NP-40-insoluble fraction but that other mitochondrial matrix proteins, P32 and mtSSB, were mostly recovered from the soluble fraction, while part of mtSSB was bound to mtDNA as a component of the mitochondrial nucleoid (1). To examine whether overexpressed TFAM is bound to mtDNA, we prepared mitochondria from MTF and HΔC cells cultured without doxycycline and then separated them into NP-40-insoluble (P1) and -soluble (S1) fractions (Fig. 7, lanes 2 to 3 and 11 to 12). As reported previously (1), most of the endogenous human TFAM (arrowhead) was recovered from the P1 fraction (Fig. 7, lanes 2 and 11), whereas most of the p32 and mtSSB were recovered from the S1 fraction (Fig. 7, lanes 3 and 12). Mitochondrial DNA was detected only in the P1 fraction by PCR (lanes 2 and 11). Both mouse TFAM-HA (double arrowheads) and human TFAM-ΔC-HA (triple arrowheads) were also mostly recovered from the P1 fraction (Fig. 7, compare lane 2 with 3 and lane 11 with 12).

The P1 fractions were treated with nuclease S7 or DNase-free RNase A and then separated into insoluble (P2) and soluble (S2) fractions. After treatment with nuclease S7, most of the endogenous human TFAM, exogenous mouse TFAM-HA, and human TFAM-ΔC-HA were recovered from the soluble fractions (S2) (lanes 7 and 16). However, after the RNase A treatment, the TFAMs were recovered from insoluble fractions (P2) (lanes 8 and 17). These findings suggest that both endogenous and exogenous TFAM molecules are bound to mtDNA as mitochondrial nucleoid components.

DISCUSSION

We showed that the amounts of TFAM and mtDNA were reduced in parallel (Fig. 2B). There are already two reports on suppression of TFAM in vertebrate cells: heterozygous targeted disruption of the *Tfam* gene in mice (19) and in chicken DT40 cells (22). In both cases, both TFAM and mtDNA were decreased by about 50%. These reports, however, showed only steady-state values a long time after the 50% decrease in TFAM, whereas we measured the daily change in the amount of TFAM and mtDNA after the start of RNAi treatment. In the present study, we first showed that the amount of mtDNA was strongly correlated to that of TFAM on a time scale that appears to be less than 1 day. Taking into account that the changes in TFAM and mtDNA were nearly the same at each day, mtDNA levels may reach the corresponding levels of TFAM within hours.

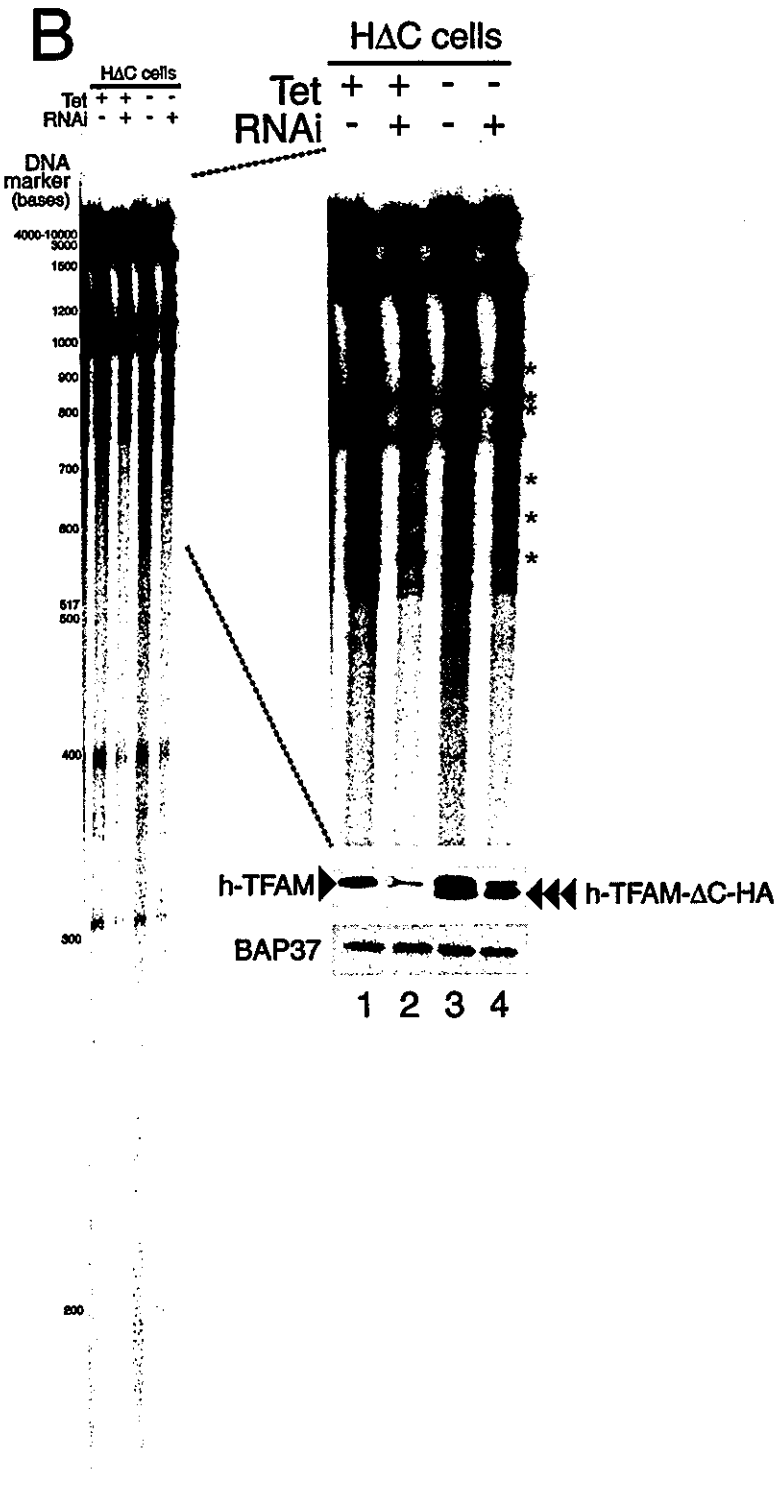

FIG. 6—*Continued*

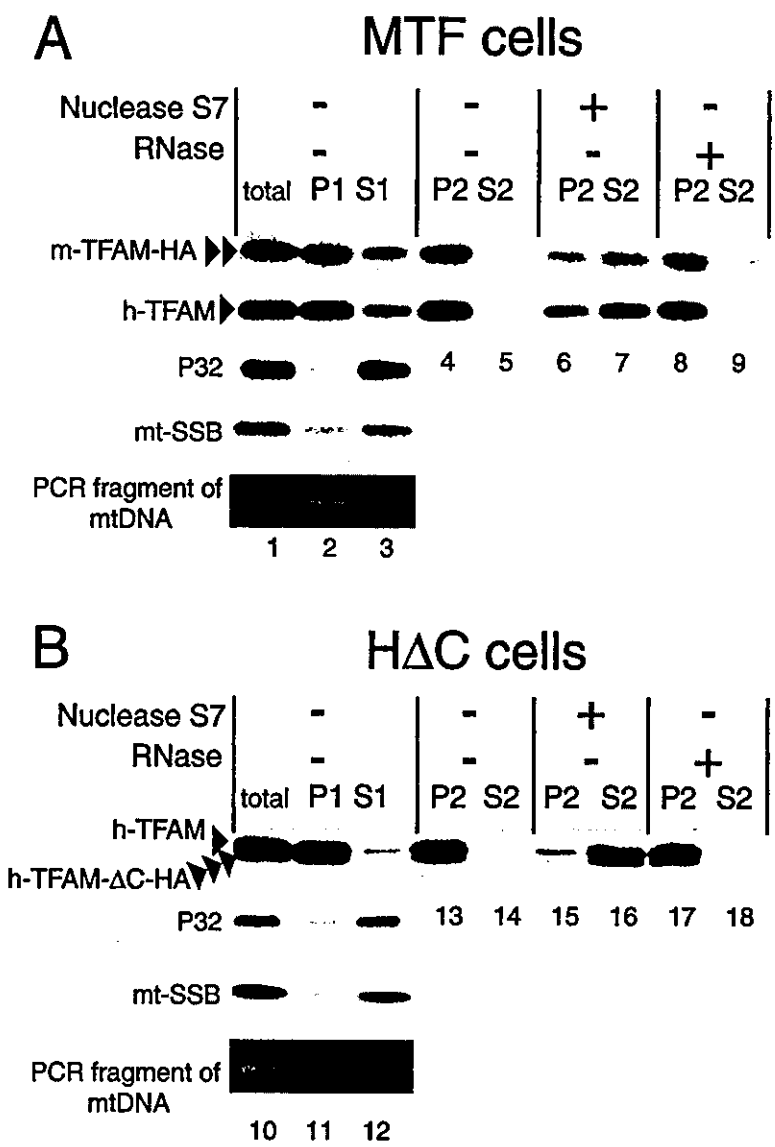

FIG. 7. Mitochondria were prepared from MTF (A) and HΔC (B) cells cultured without doxycycline. The mitochondria were solubilized with 0.5% NP-40 (total) and separated into pellet (P1) and supernatant (S1). The P1 fractions were treated with nuclease S7 or DNase-free RNase A and then separated again into pellet (P2) and supernatant (S2). Each sample was analyzed by Western blotting with anti-human TFAM, anti-P32, anti-mtSSB, and anti-HA antibodies. mtDNA in total, P1, and S1 were detected by PCR. Human TFAM (arrowhead), mouse TFAM-HA (double arrowheads), and human TFAM-ΔC-HA (triple arrowheads) are indicated.

The replication of mammalian mtDNA is coupled with transcription according to the strand displacement model (34). Thus, one possible mechanism by which mtDNA decreases or increases with the decrease or increase in TFAM is that replication of mtDNA is down- or upregulated due to the down- or upregulation of TFAM-activated transcription. However, we found that the transcription level was not correlated with the amount of mtDNA (Fig. 5C and 6B). On the other hand, we noticed a striking correlation between the levels of TFAM and mtDNA. TFAM is a transcription factor (10, 11, 23, 30), but it is also an HMG protein having DNA-binding properties regardless of DNA sequence (11, 30). TFAM molecules are abundant enough to cover mtDNA entirely, and indeed most of them bind mtDNA, suggesting that mtDNA is packaged with TFAM (1, 36) and TFAM is in functional excess (33).

Such a nucleoid structure may also be required for the stability of mtDNA. In agreement with this notion, mouse TFAM and human TFAM-ΔC were as active in the maintenance of mtDNA as wild-type TFAM, at least under conditions in which promoter-specific transcription was maintained at a certain level (Fig. 5C and 6B). About 85% of full-length TFAM could be replaced without reduction in mtDNA by TFAM-ΔC-HA, which has only 1% of the LSP-dependent transcription activity of full-length TFAM (Fig. 5A and C). If the majority of TFAM

molecules maintained mtDNA through transcription-coupled replication, the amount of mtDNA would decrease. Therefore, this result raises the possibility that the majority of TFAM molecules participate architecturally in maintenance.

The overexpressed recombinant TFAM was mostly recovered from the insoluble fraction together with mtDNA (Fig. 7, lanes 2 and 11). Nuclease S7 treatment but not RNase A treatment released recombinant TFAM as well as endogenous TFAM to the soluble fraction (Fig. 7, lanes 6 to 9 and 15 to 18), supporting the idea of TFAM-mtDNA binding. Taken together with the fact that the level of mtDNA rapidly and finely corresponds to the level of TFAM (Fig. 2), one likely explanation is that the vast majority of TFAM molecules are bound to mtDNA and that only mtDNA covered with TFAM can be maintained. According to this model, the mass but not the copy number of mtDNA would be titrated by TFAM, consistent with a finding by Tang et al. that the total mass but not the copy number of mtDNA is constant among cells harboring wild-type, deleted, and partially duplicated mtDNAs (37). Conversely, when mtDNA was depleted with ethidium bromide in HeLa cells, TFAM was reduced to the same extent as mtDNA (33). TFAM and mtDNA may thus stabilize each other when bound together.

We presume that TFAM exists abundantly and that the majority of TFAM molecules are bound to sites other than the promoter regions for packaging mtDNA. Goto et al. reported that TFAM levels can be substantially reduced by RNAi without significant inhibition of transcription per mtDNA in insect cells (15). Here we also showed that transcription per mtDNA was not decreased but rather upregulated by RNAi-induced suppression of TFAM (see Fig. 5C and Fig. 6B, lane 2). These observations suggest that the amount of TFAM can be reduced without lowering the transcription level per mtDNA if the amount of TFAM is manipulated within a cell. In contrast, Garstka et al. reported that import of TFAM into isolated mitochondria significantly enhances transcription in organello (14).

The reason for these apparently contradictory observations is currently unknown. However, the differences may reflect differences in the experimental systems. Garstka et al. manipulated the amount of TFAM with isolated mitochondria, while we in the present study and Goto et al. did so in living cells. A possible but hypothetical explanation is to assume that TFAM preferentially binds to promoters with a higher affinity but can also be preferentially displaced from the promoters by an unknown mechanism. In a cell, continuous input of TFAM would compensate for this selective displacement. However, in isolated mitochondria, there is no input of TFAM unless TFAM is imported artificially, as done by Garstka et al. When the promoter regions are selectively vacant at a certain level, a small amount of TFAM could enhance transcription because TFAM has a higher affinity for the promoters. A human Lon protease homologue is one candidate for such selective displacement, because the homologue was recently reported to bind preferentially to the GT-rich sequence overlapping the LSP of human mtDNA (21).

TFAM is essential for transcription of mtDNA, and TFAM-enabled transcription may be involved in the replication of mtDNA. However, we propose that TFAM may have a dual role in the maintenance of mtDNA, transcription and nucleoid formation. It is probable that the majority of TFAM molecules are involved in architecturally maintaining the higher structure of mtDNA, because at any time most TFAM molecules should be bound to nonpromoter regions. The higher structure is called nucleoid in general. However, it might be more appropriately described as a mitochondrial chromosome or mitochromosome when based on the whole structure of mtDNA.

ACKNOWLEDGMENTS

This work was supported in part by the Uehara Memorial Foundation, the Naito Foundation, and Grants-in-Aid for Scientific Research from the Ministry of Education, Science, Technology, Sports and Culture of Japan.

We extend special thanks to Eric A. Schon (Department of Genetics and Development and Neurology, Columbia University) for critical discussion. We are grateful to Keiji Hisaeda (Department of Medical Biochemistry, Kyushu University) for useful technical advice.

REFERENCES

1. **Alam, T. I., T. Kanki, T. Muta, K. Ukaji, Y. Abe, H. Nakayama, K. Takio, N. Hamasaki, and D. Kang.** 2003. Human mitochondrial DNA is packaged with TFAM. Nucleic Acids Res. **31**:1640–1645.
2. **Albring, M., J. Griffith, and G. Attardi.** 1977. Association of a protein structure of probable membrane derivation with HeLa cell mitochondrial DNA near its origin of replication. Proc. Natl. Acad. Sci. USA **74**:1348–1352.
3. **Barat, M., D. Rickwood, C. Dufresne, and J. C. Mounolou.** 1985. Characterization of DNA-protein complexes from the mitochondria of Xenopus laevis oocytes. Exp. Cell Res. **157**:207–217.
4. **Bowmaker, M., M. Y. Yang, T. Yasukawa, A. Reyes, H. T. Jacobs, J. A. Huberman, and I. J. Holt.** 2003. Mammalian mitochondrial DNA replicates bidirectionally from an initiation zone. J. Biol. Chem. **278**:50961–50969.
5. **Caron, F., C. Jacq, and J. Rouviere-Yaniv.** 1979. Characterization of a histone-like protein extracted from yeast mitochondria. Proc. Natl. Acad. Sci. USA **76**:4265–4269.
6. **Dairaghi, D. J., G. S. Shadel, and D. A. Clayton.** 1995. Addition of a 29 residue carboxyl-terminal tail converts a simple HMG box-containing protein into a transcriptional activator. J. Mol. Biol. **249**:11–28.
7. **DeFrancesco, L., and G. Attardi.** 1981. In situ photochemical crosslinking of HeLa cell mitochondrial DNA by a psoralen derivative reveals a protected region near the origin of replication. Nucleic Acids Res. **9**:6017–6030.
8. **Diffley, J. F., and B. Stillman.** 1992. DNA binding properties of an HMG1-related protein from yeast mitochondria. J. Biol. Chem. **267**:3368–3374.
9. **Enriquez, J. A., A. Perez-Martos, M. J. Lopez-Perez, and J. Montoya.** 1996. In organello RNA synthesis system from mammalian liver and brain. Methods Enzymol. **264**:50–57.
10. **Falkenberg, M., M. Gaspari, A. Rantanen, A. Trifunovic, N. G. Larsson, and C. M. Gustafsson.** 2002. Mitochondrial transcription factors B1 and B2 activate transcription of human mtDNA. Nat. Genet. **31**:289–294.
11. **Fisher, R. P., and D. A. Clayton.** 1988. Purification and characterization of human mitochondrial transcription factor 1. Mol. Cell. Biol. **8**:3496–3509.
12. **Fisher, R. P., T. Lisowsky, M. A. Parisi, and D. A. Clayton.** 1992. DNA wrapping and bending by a mitochondrial high mobility group-like transcriptional activator protein. J. Biol. Chem. **267**:3358–3367.
13. **Garrido, N., L. Griparic, E. Jokitalo, J. Wartiovaara, A. M. van der Bliek, and J. N. Spelbrink.** 2003. Composition and dynamics of human mitochondrial nucleoids. Mol. Biol. Cell **14**:1583–1596.
14. **Garstka, H. L., W. E. Schmitt, J. Schultz, B. Sogl, B. Silakowski, A. Perez-Martos, J. Montoya, and R. J. Wiesner.** 2003. Import of mitochondrial transcription factor A (TFAM) into rat liver mitochondria stimulates transcription of mitochondrial DNA. Nucleic Acids Res. **31**:5039–5047.
15. **Goto, A., Y. Matsushima, T. Kadowaki, and Y. Kitagawa.** 2001. Drosophila mitochondrial transcription factor A (d-TFAM) is dispensable for the transcription of mitochondrial DNA in Kc167 cells. Biochem. J. **354**:243–248.
16. **Holt, I. J., H. E. Lorimer, and H. T. Jacobs.** 2000. Coupled leading- and lagging-strand synthesis of mammalian mitochondrial DNA. Cell **100**:515–524.
17. **Kaufman, B. A., S. M. Newman, R. L. Hallberg, C. A. Slaughter, P. S. Perlman, and R. A. Butow.** 2000. In organello formaldehyde crosslinking of proteins to mtDNA: identification of bifunctional proteins. Proc. Natl. Acad. Sci. USA **97**:7772–7777.
18. **Kozak, M.** 1989. Context effects and inefficient initiation at non-AUG codons in eucaryotic cell-free translation systems. Mol. Cell. Biol. **9**:5073–5080.
19. **Larsson, N. G., J. Wang, H. Wilhelmsson, A. Oldfors, P. Rustin, M. Lewandoski, G. S. Barsh, and D. A. Clayton.** 1998. Mitochondrial transcription factor A is necessary for mtDNA maintenance and embryogenesis in mice. Nat. Genet. **18**:231–236.
20. **Lee, D. Y., and D. A. Clayton.** 1998. Initiation of mitochondrial DNA replication by transcription and R-loop processing. J. Biol. Chem. **273**:30614–30621.